

Quantum Fluids and Solids

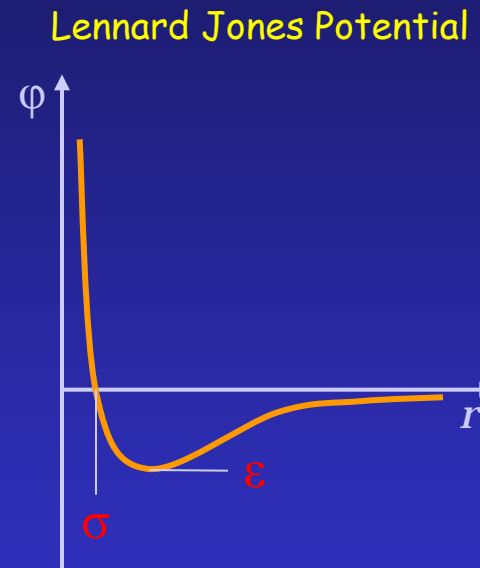
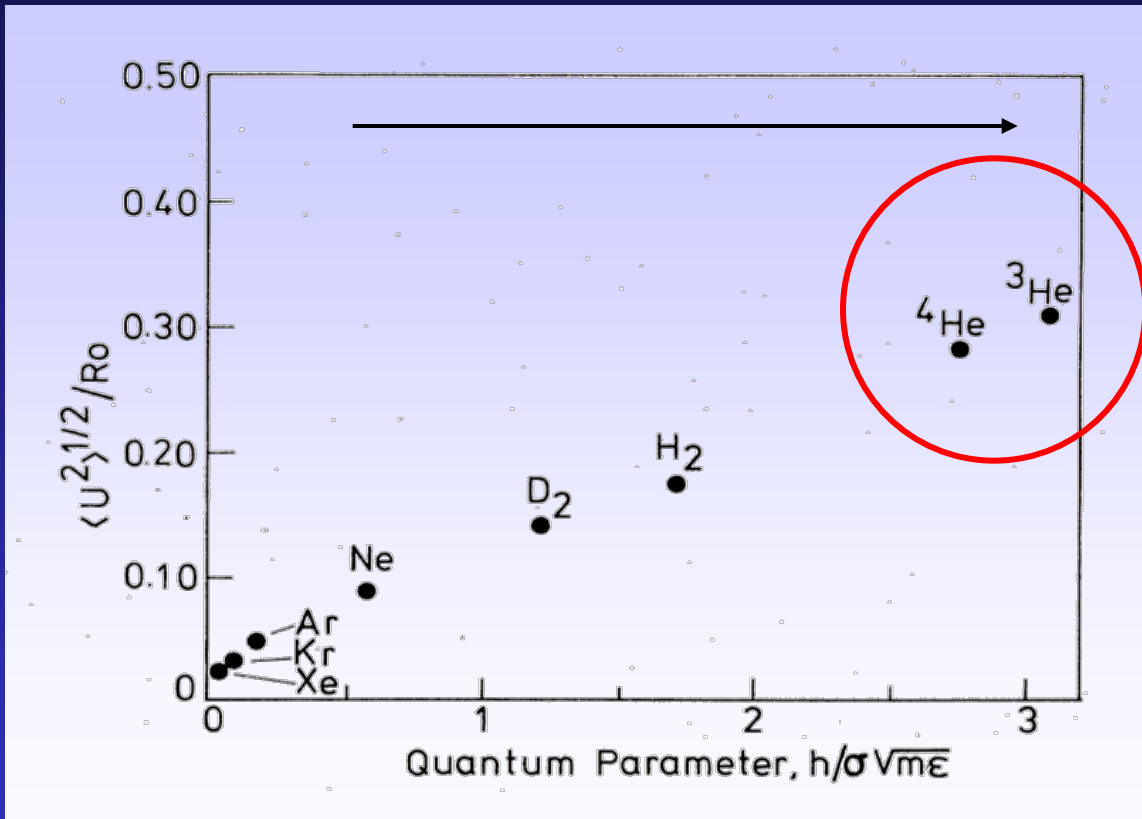
Christian Enss (4He) & Henri Godfrin (3He)



J. Allen 1970

Chichilianne 2011

What Do We Consider as Quantum Matter ?



De Boer quantum parameter: $\Lambda^* = \frac{\Lambda_B}{\sigma} = \frac{h}{\sigma\sqrt{2m\varepsilon}}$

De Broglie wavelength: $\Lambda_B = \frac{h}{p}$

Overview

Introduction

Phase Diagrams

He-II Experimental Observations

Superfluidity

Viscosity

Second sound

Two Fluid Model

Hydrodynamics

Thermodynamical effect

Sound propagation

Bose-Einstein Condensate

Condensate fraction

Macroscopic wave function

Quantized vortices

Normal Fluid Component

Excitation spectrum

Critical Velocity

Quantum Crystals

Fermions: ^3He

Phase diagram

Melting curve

Normal Fluid ^3He

Fermi liquids

Heat capacity

Magnetic susceptibility

Superfluid ^3He

Cooper pairs

A and B phases

Vortices

Dirac multi-spin exchange

U2D2 phase

CNAF phase

Susceptibility and heat capacity

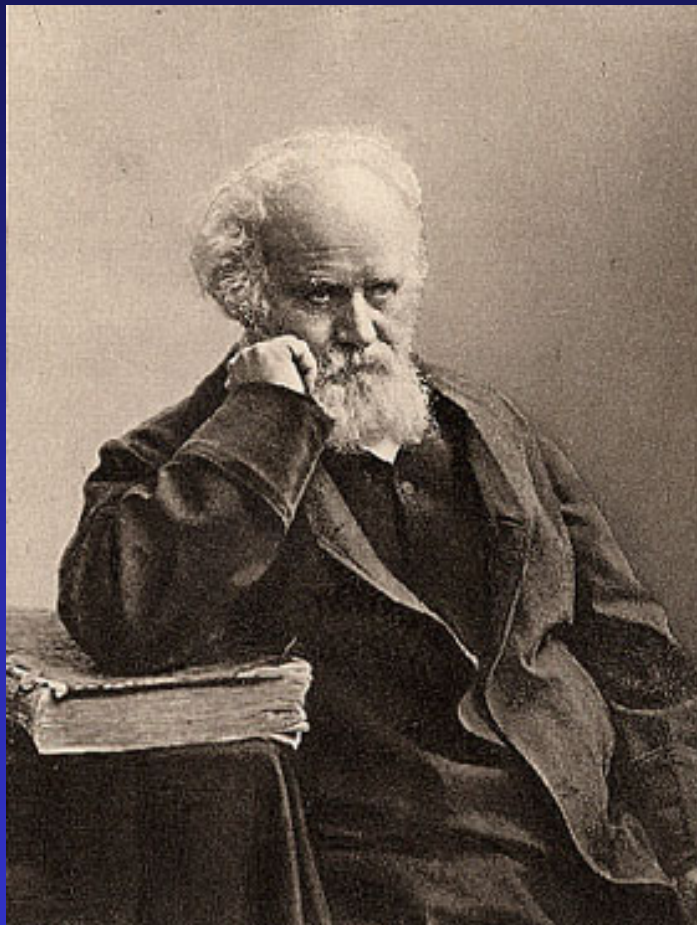
2D Systems

Heisenberg ferromagnet

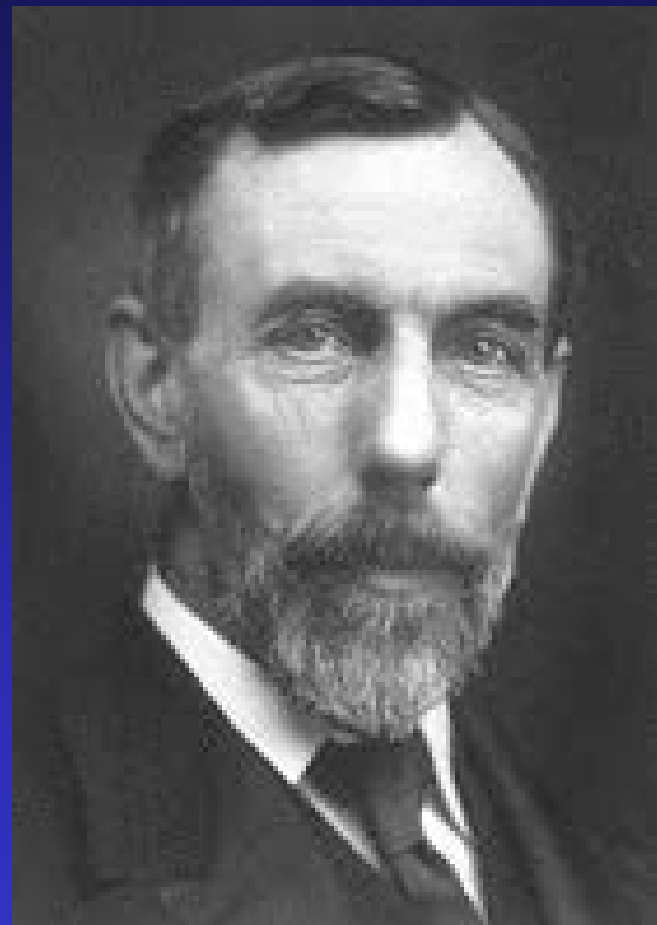
Spin liquid

Conclusions

Discovery of Helium

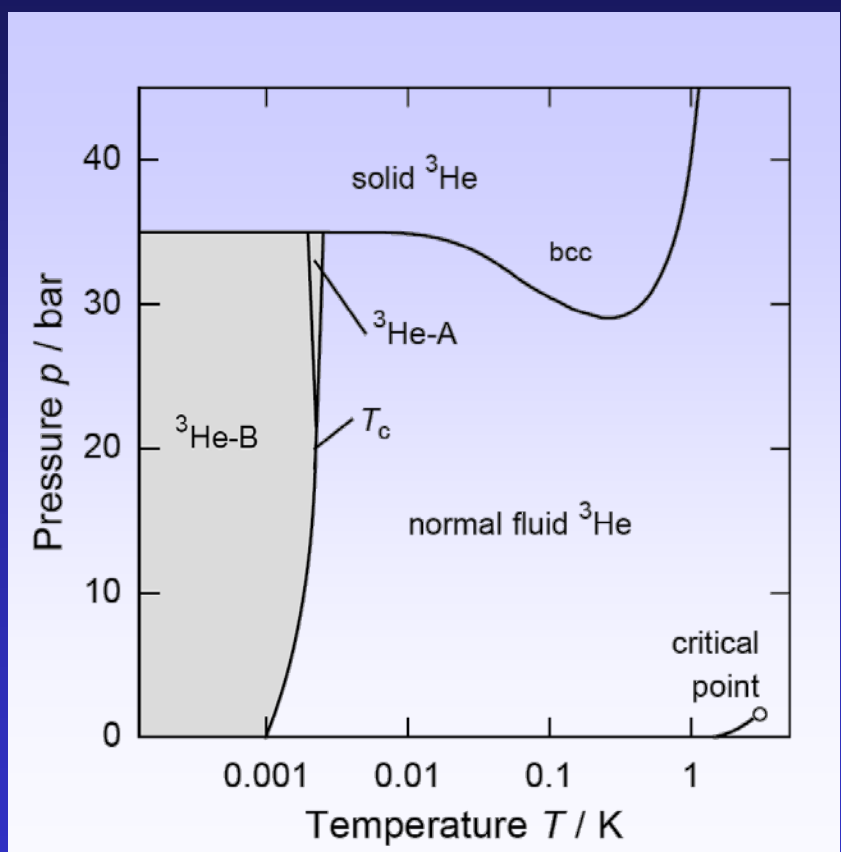
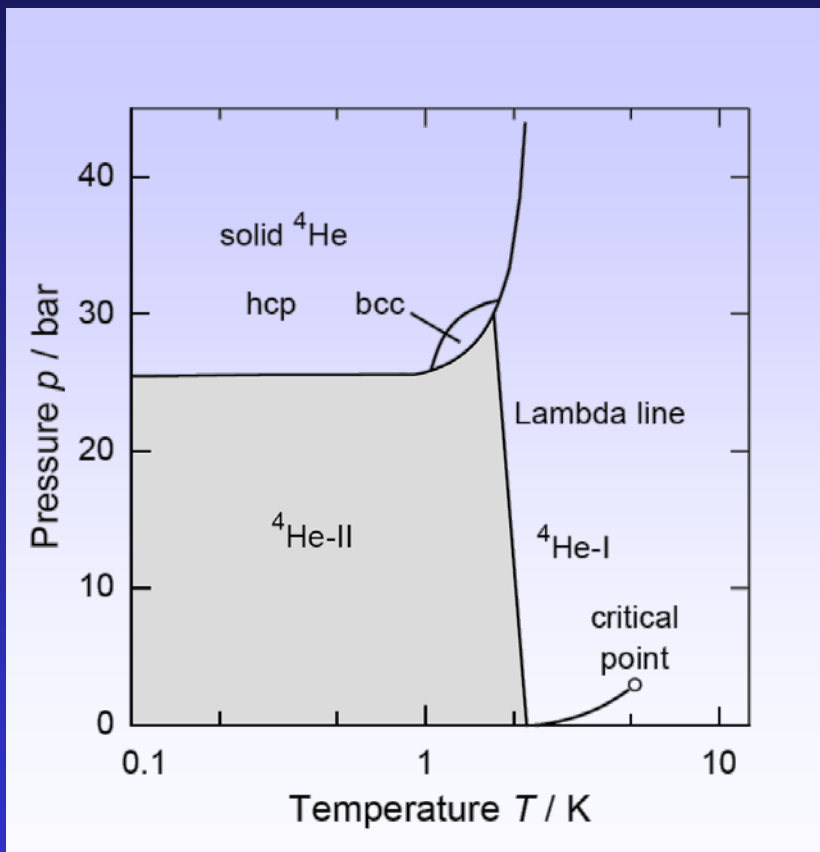


Pierre Jules César Janssen



Sir William Ramsay

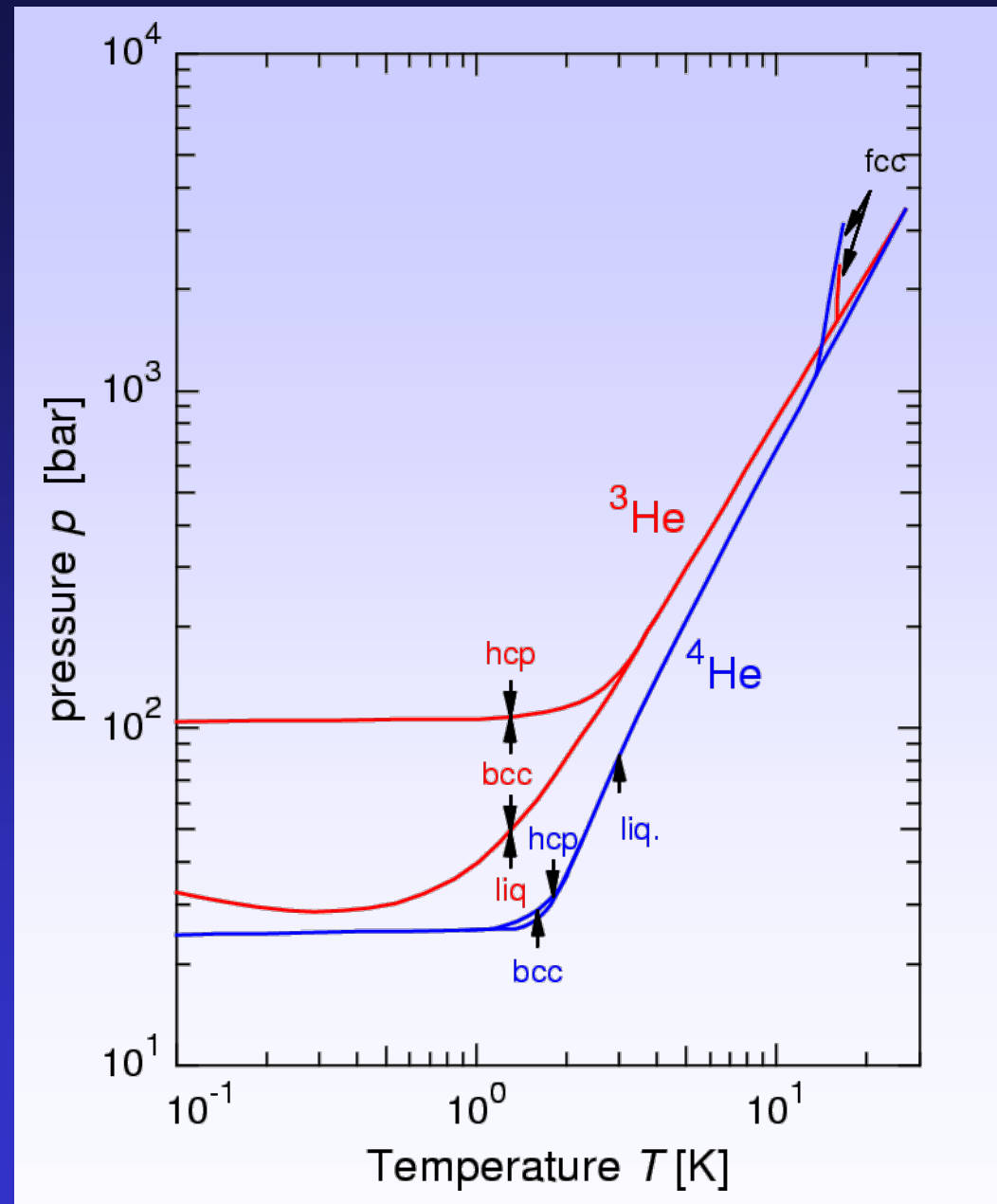
Phase Diagrams of ^3He and ^4He



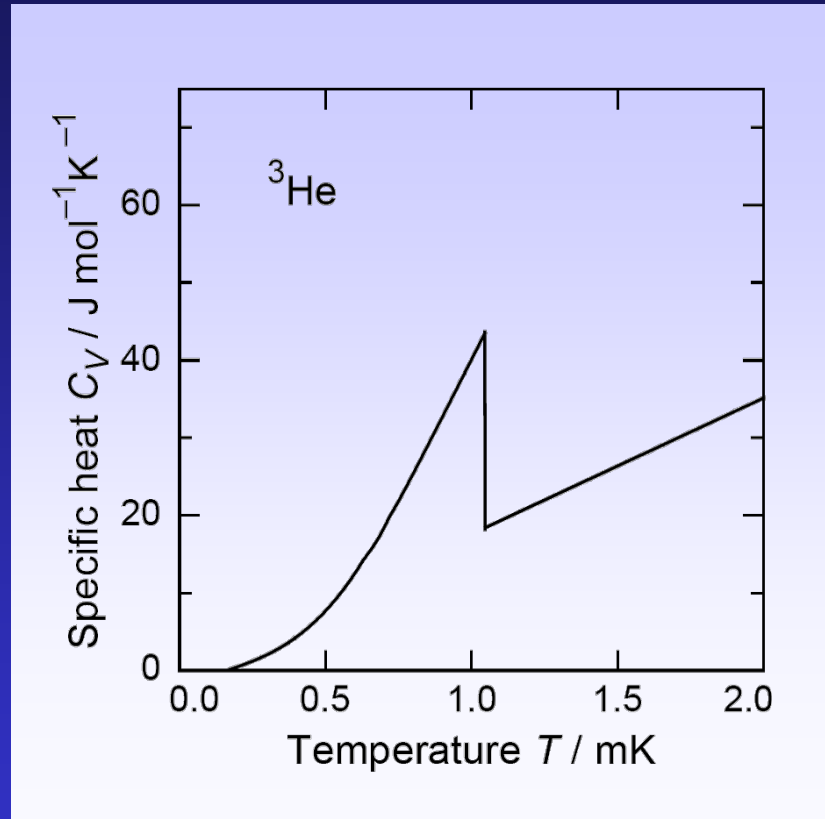
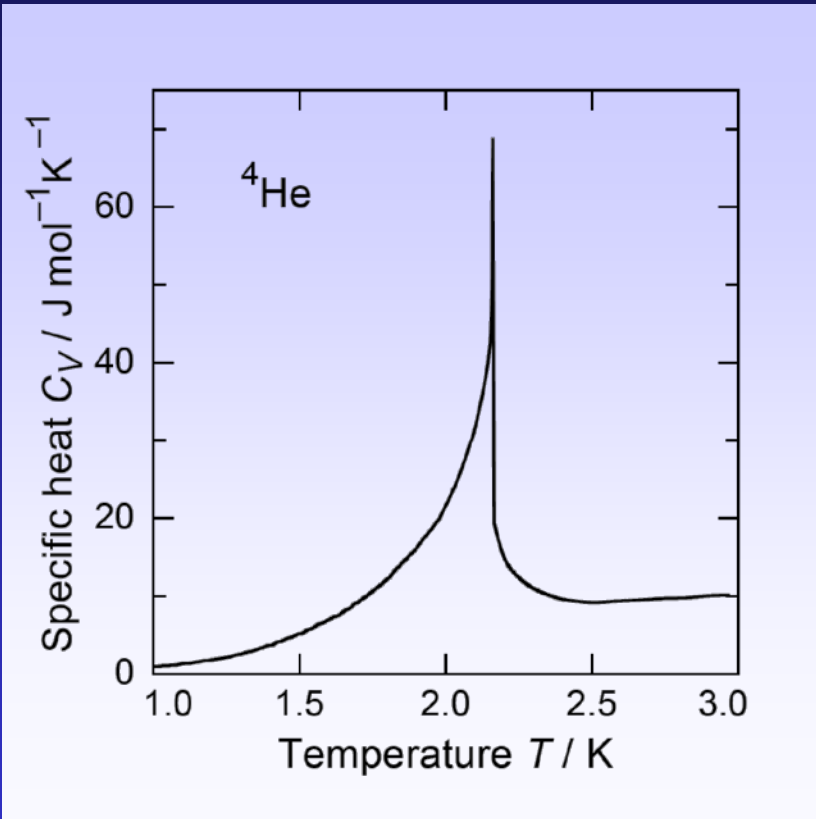
Solid Phases

bcc phase much larger for ^3He
→ less dense because of
higher zero point energy

zero point energy unimportant
at high temperatures



Specific Heat at the Superfluid Transition



Superfluidity: Flow Through Thin Capillaries

Hagen-Poiseuille law

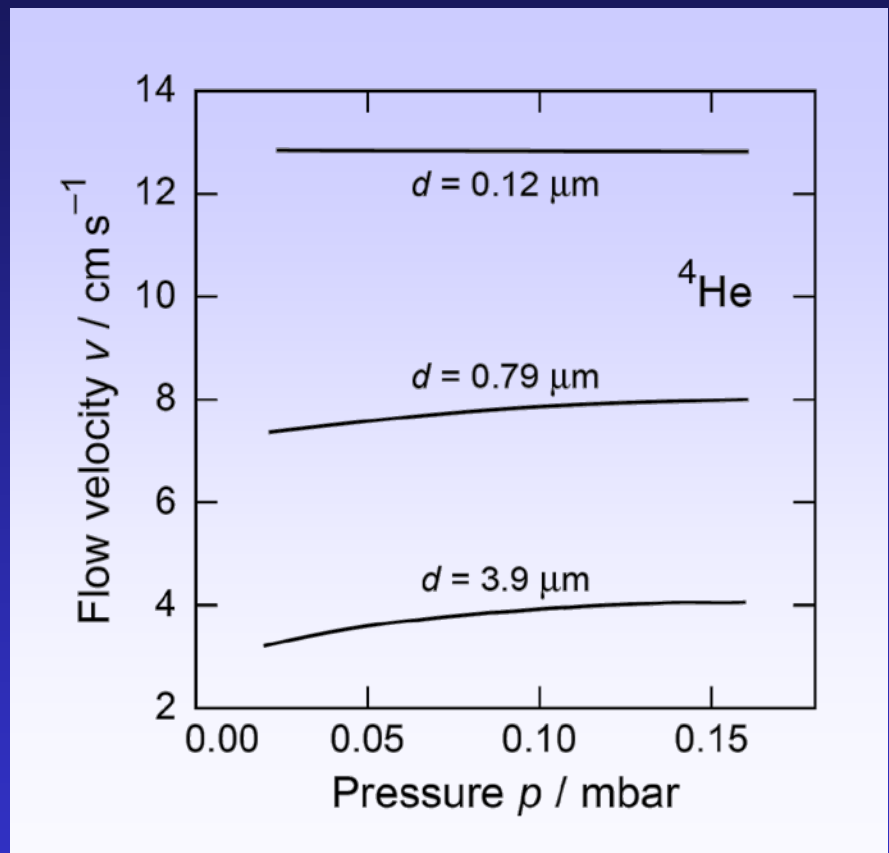
$$\dot{V} = \frac{\pi r^4}{8} \frac{1}{\eta} \frac{\Delta p}{L}$$

Flow velocity

$$v = \dot{V} / (\pi r^2)$$

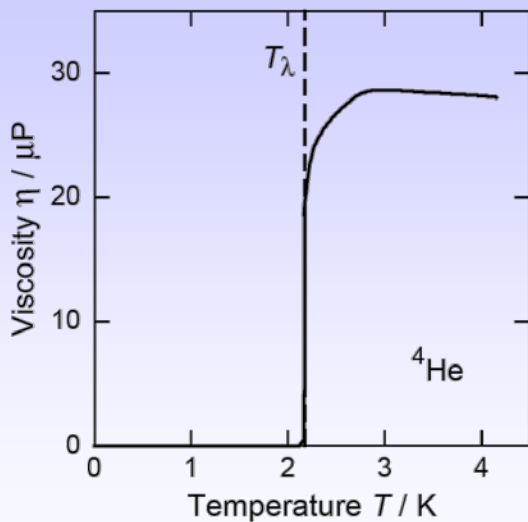
Experimental result:

flow velocity is independent of pressure
and increases with decreasing diameter

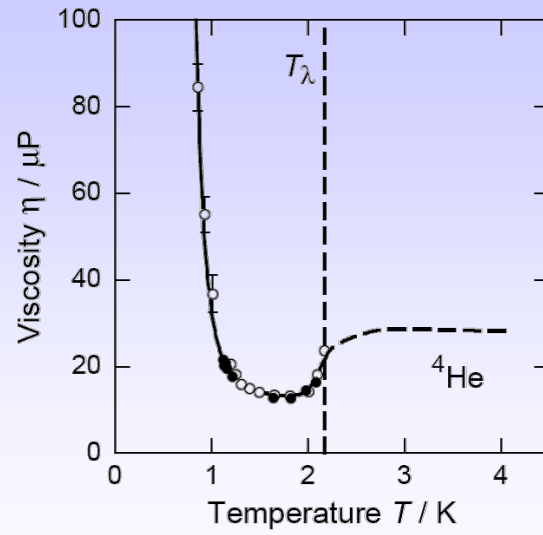


Temperature Dependence of Viscosity

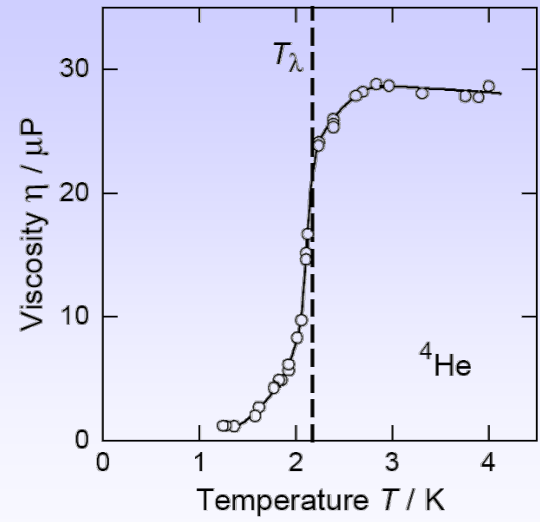
flow through capillary



rotary viscosimeter

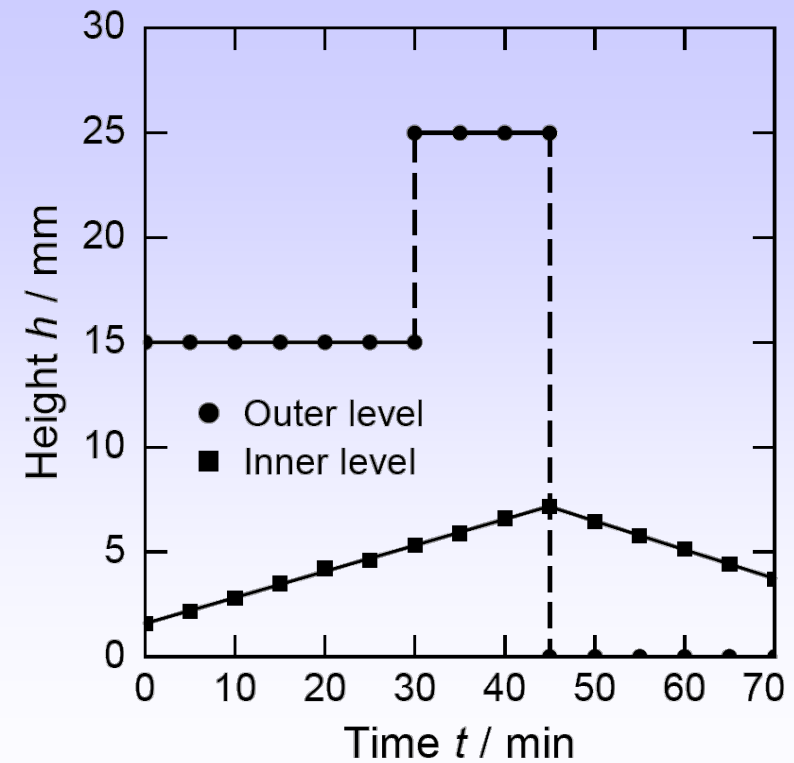
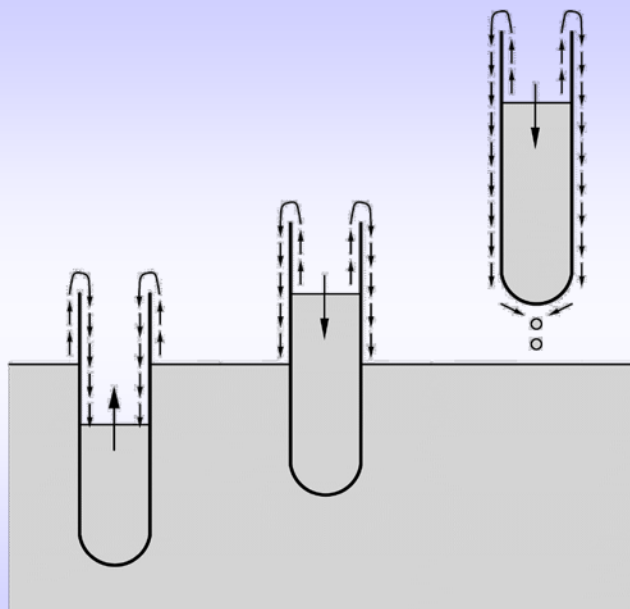


oscillating disc

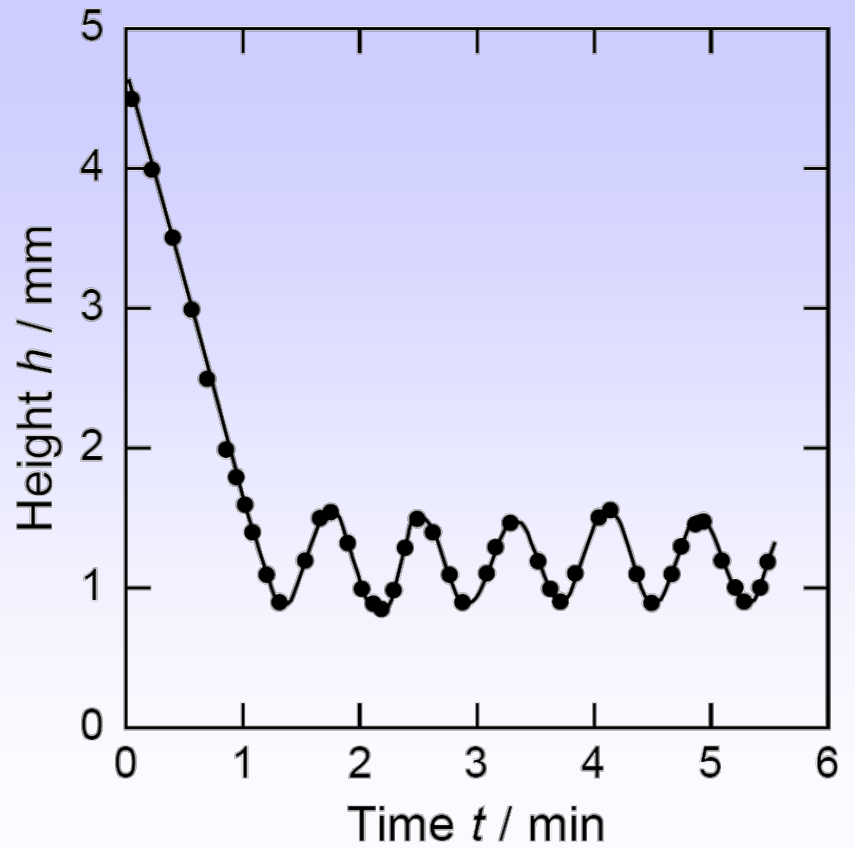
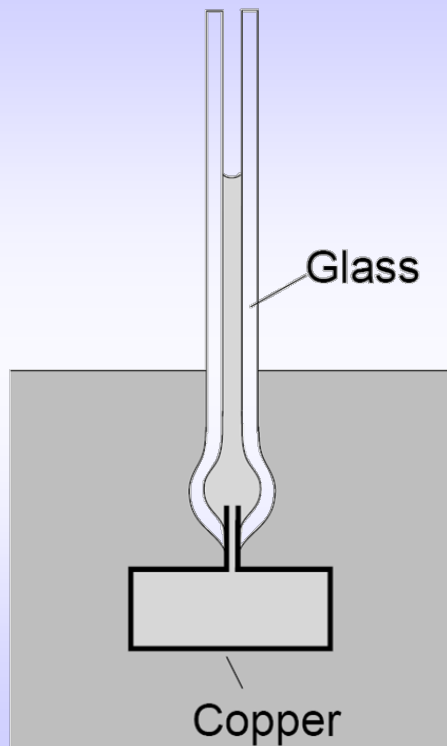


Three different results and all experiments are correct! What is wrong?

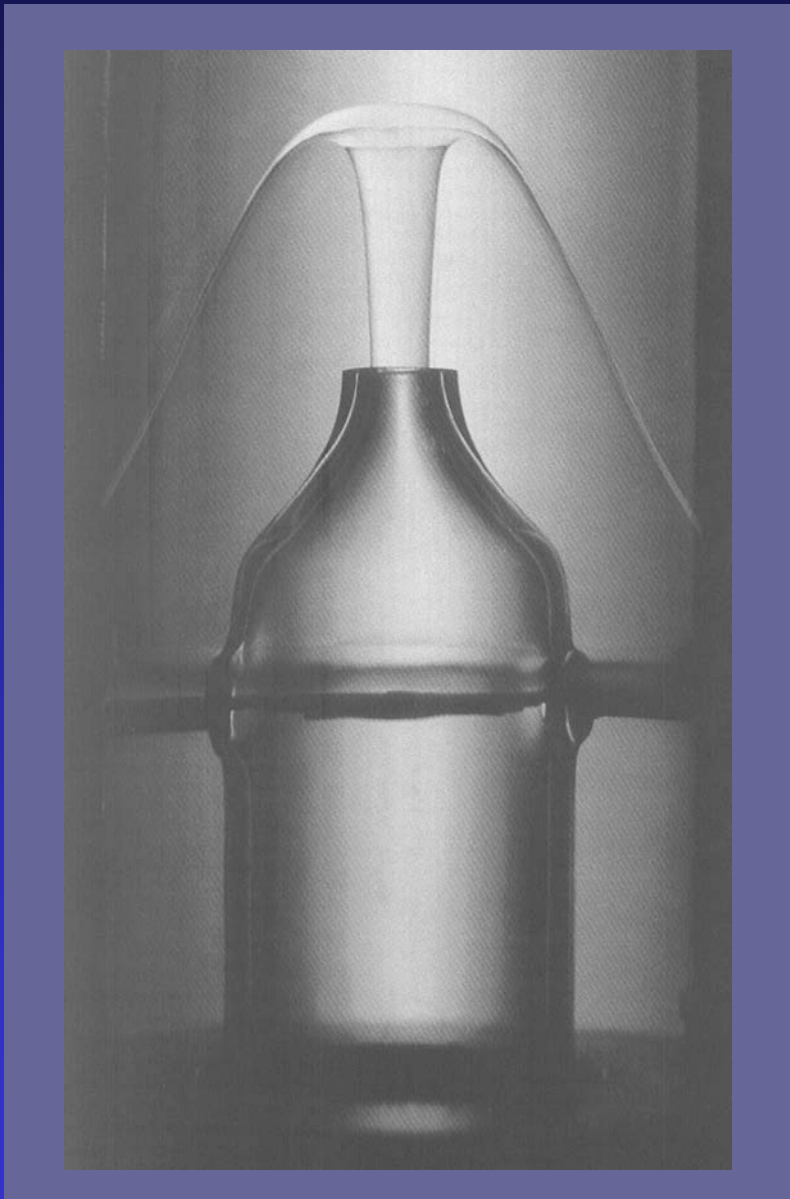
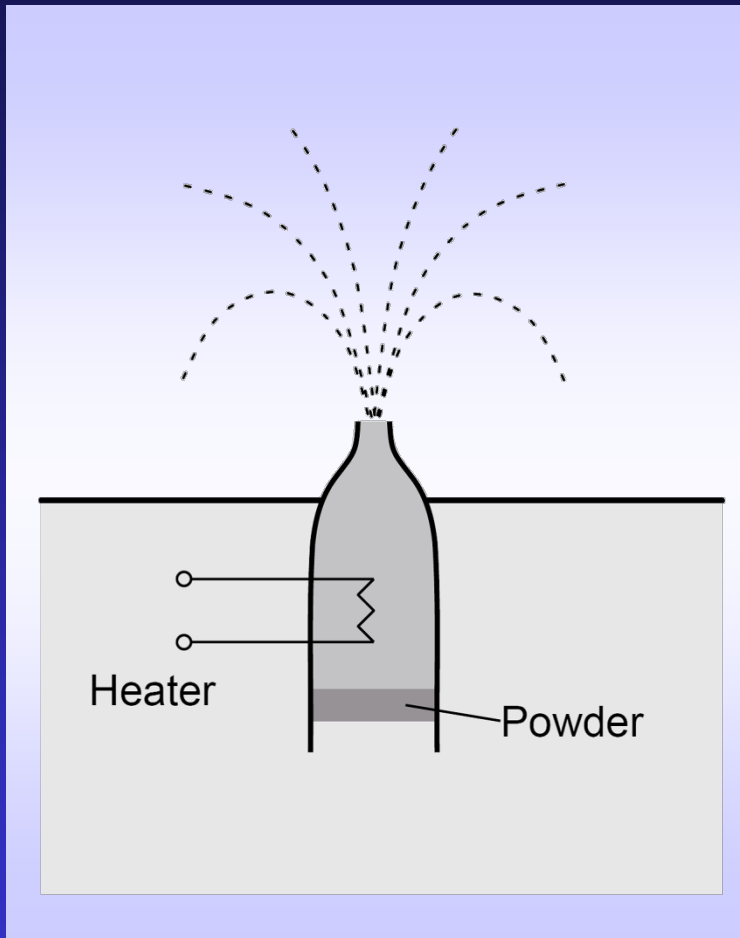
Beaker Experiments



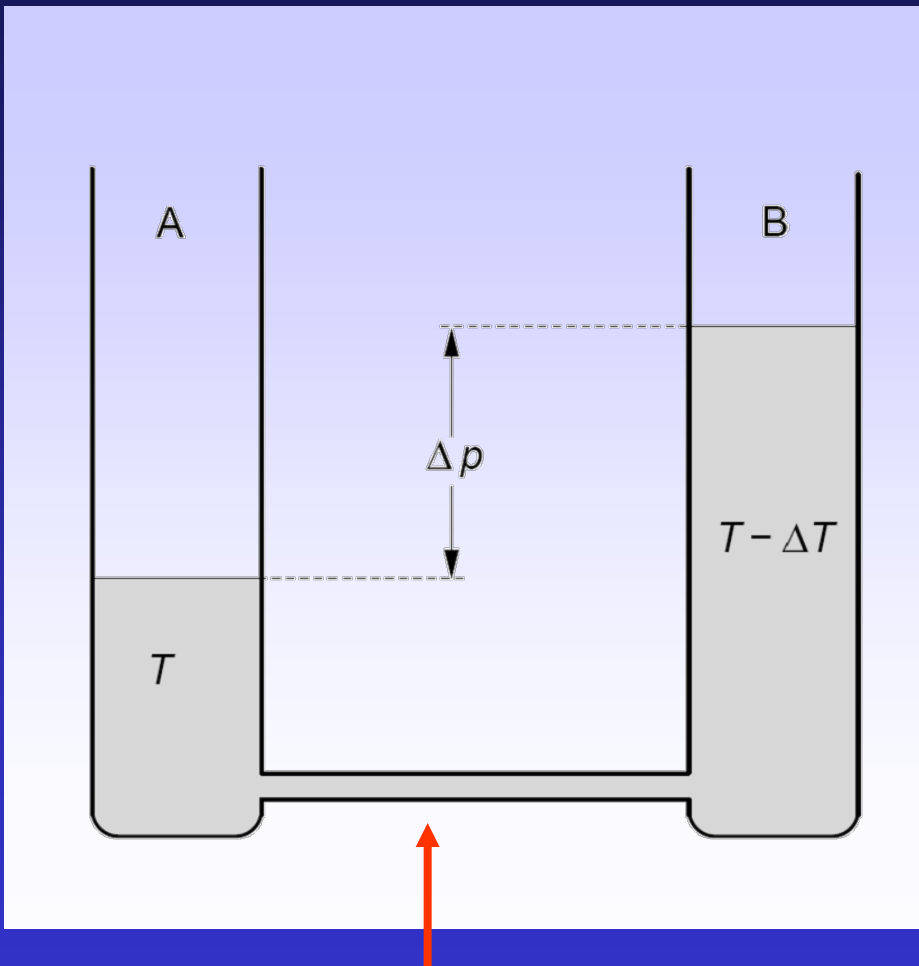
Beaker Experiments



Fountain Effect



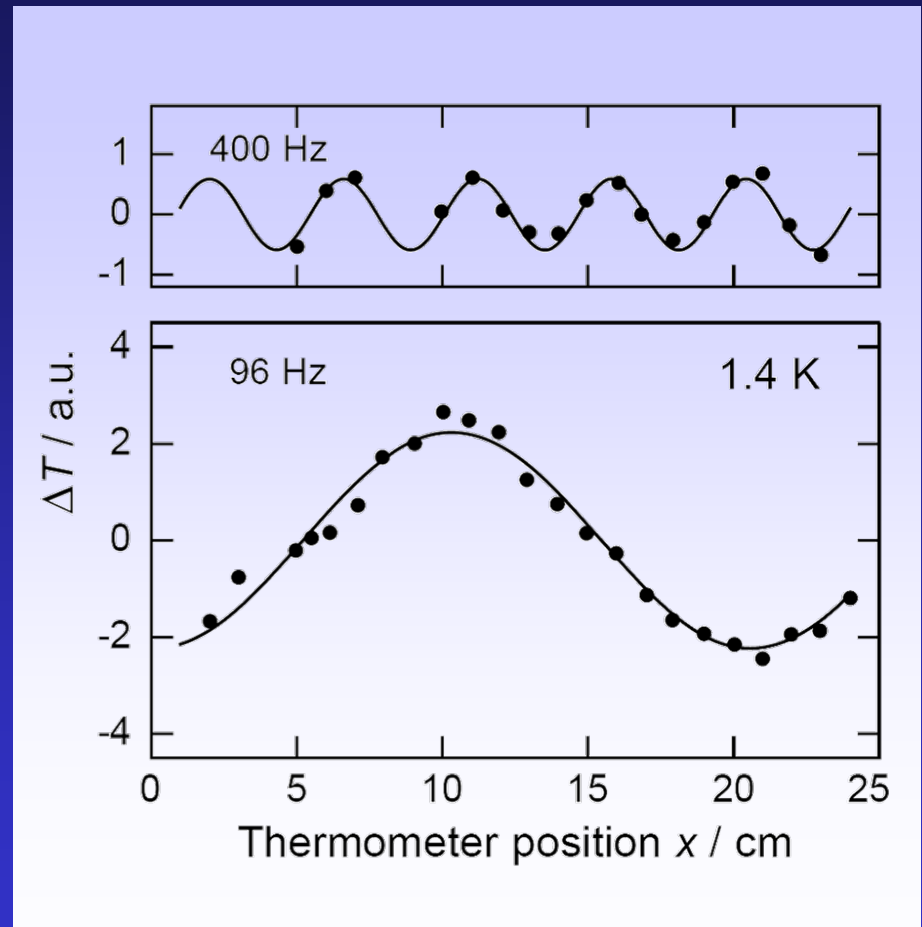
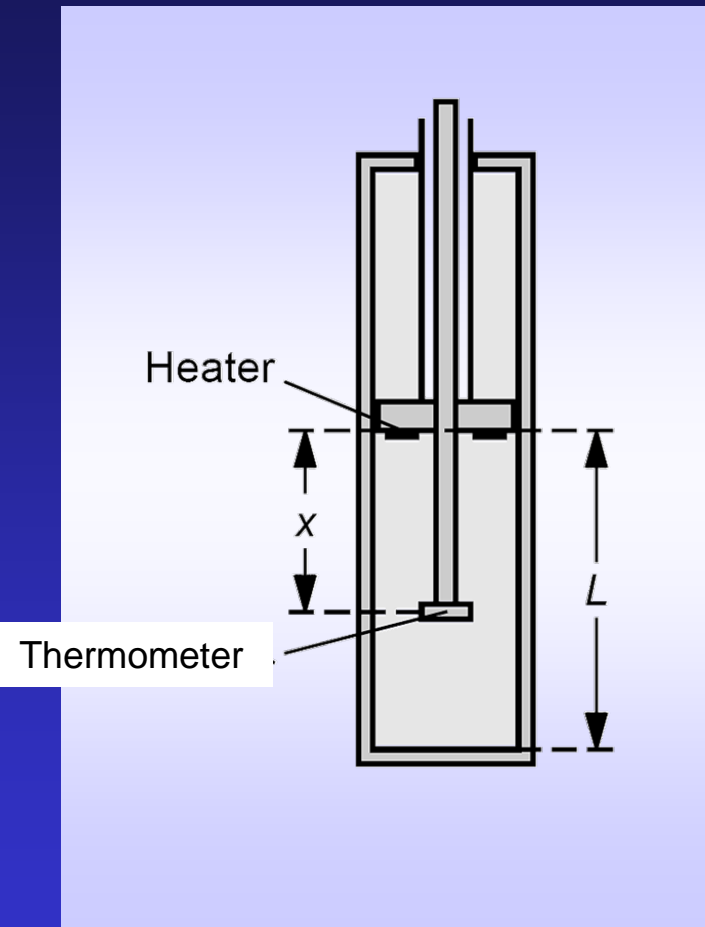
Thermomechanical Effect



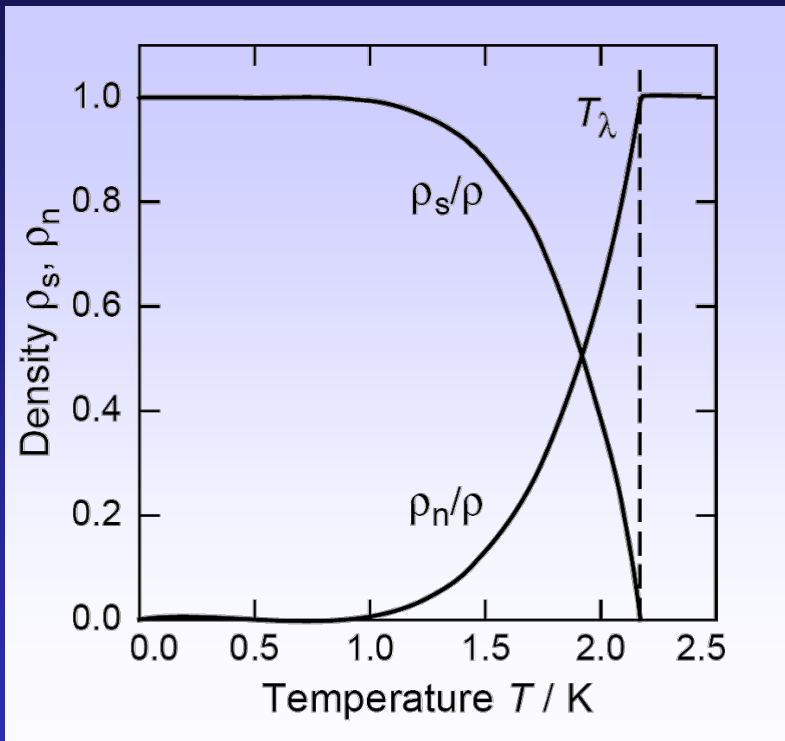
very thin capillary (superleak)

direction of mass transport
is opposite to heat transport

Second Sound: Temperature waves



Two Fluid Model



basic idea

$$\varrho = \varrho_n + \varrho_s$$

$$T = T_\lambda$$

$$\varrho_s = 0 \quad \varrho_n = \varrho$$

$$T = 0$$

$$\varrho_s = \varrho \quad \varrho_n = 0$$

	density	viscosity	entropy
normal fluid component	ϱ_n	$\eta_n = \eta$	$S_n = S$
suprafluid component	ϱ_s	$\eta_s = 0$	$S_s = 0$

Two Fluid Hydrodynamics

mass flow

$$\mathbf{j} = \varrho_n \mathbf{v}_n + \varrho_s \mathbf{v}_s$$

mass conservation

$$\frac{\partial \varrho}{\partial t} = -\operatorname{div} \mathbf{j}$$

Euler equation

$$\frac{\partial \mathbf{j}}{\partial t} + \underbrace{\varrho \mathbf{v} \cdot \operatorname{grad} \mathbf{v}}_{\approx 0} = -\operatorname{grad} p$$

entropy conservation

$$\frac{\partial (\varrho S)}{\partial t} = -\operatorname{div}(\varrho S \mathbf{v}_n)$$

equation of motion
superfluid component

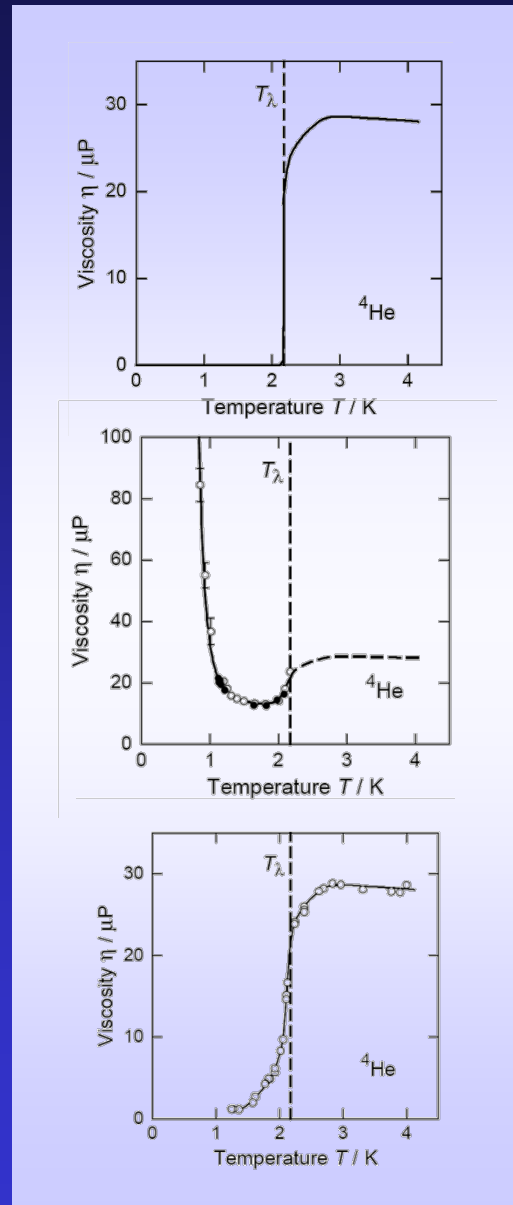
$$\frac{\partial \mathbf{v}_s}{\partial t} = S \operatorname{grad} T - \frac{1}{\varrho} \operatorname{grad} p$$

Viscosity Experiments

Flow Through Capillaries:

Superfluid component is flowing at critical velocity

→ no viscosity below Lambda point



Rotary Viscosimeter:

$$\text{Torque: } M_r = \pi \eta \omega d_r^2 d_s^2 / (d_s^2 - d_r^2)$$

Normal fluid component is observed below Lambda point

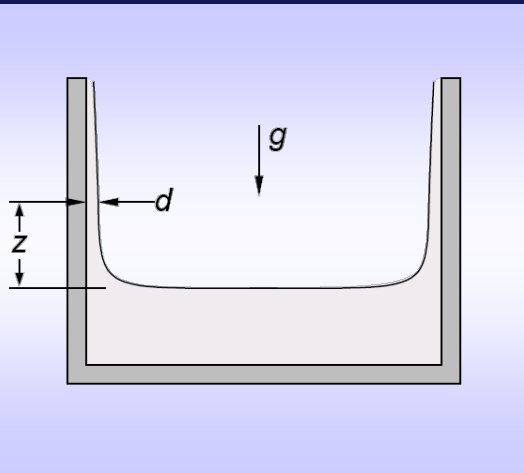
→ viscosity depends on mean free path of excitations

Oscillating Disc Viscosimeter:

$$\text{Torque: } M_d = \pi \sqrt{\rho \eta} \omega^{3/2} r^4 \Theta(\omega)$$

Product of normal fluid density and normal fluid viscosity is observed

Beaker flow: Helium films

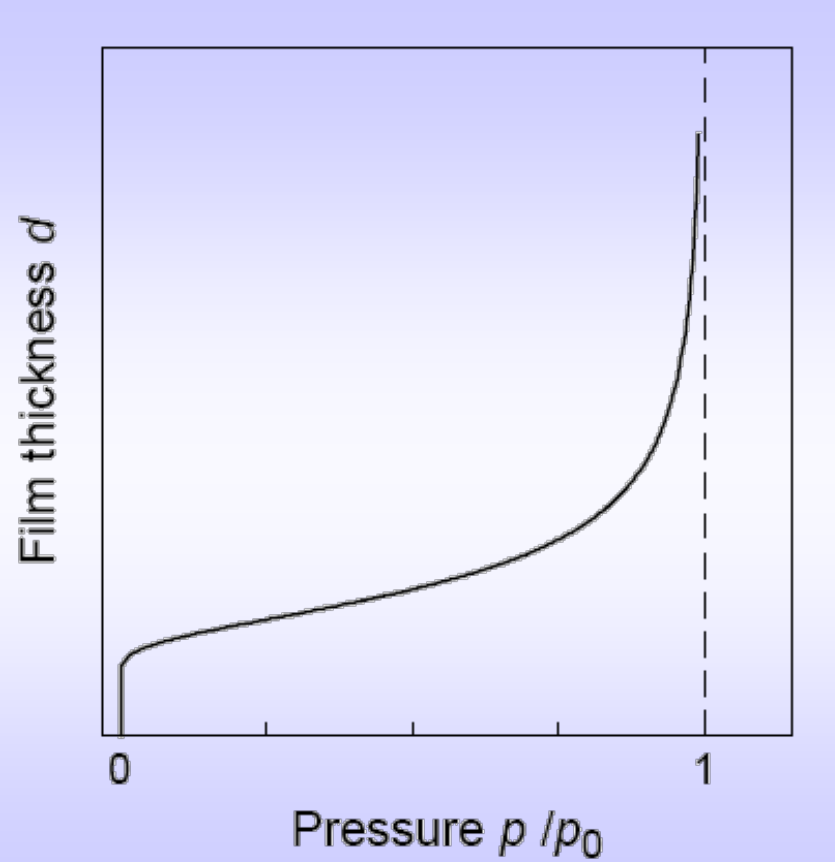


Film thickness at saturated vapor:

$$d = \sqrt[3]{\frac{\alpha}{gz}}$$

For $z = 10 \text{ cm}$

→ 200 \AA



Film flows at the critical velocity

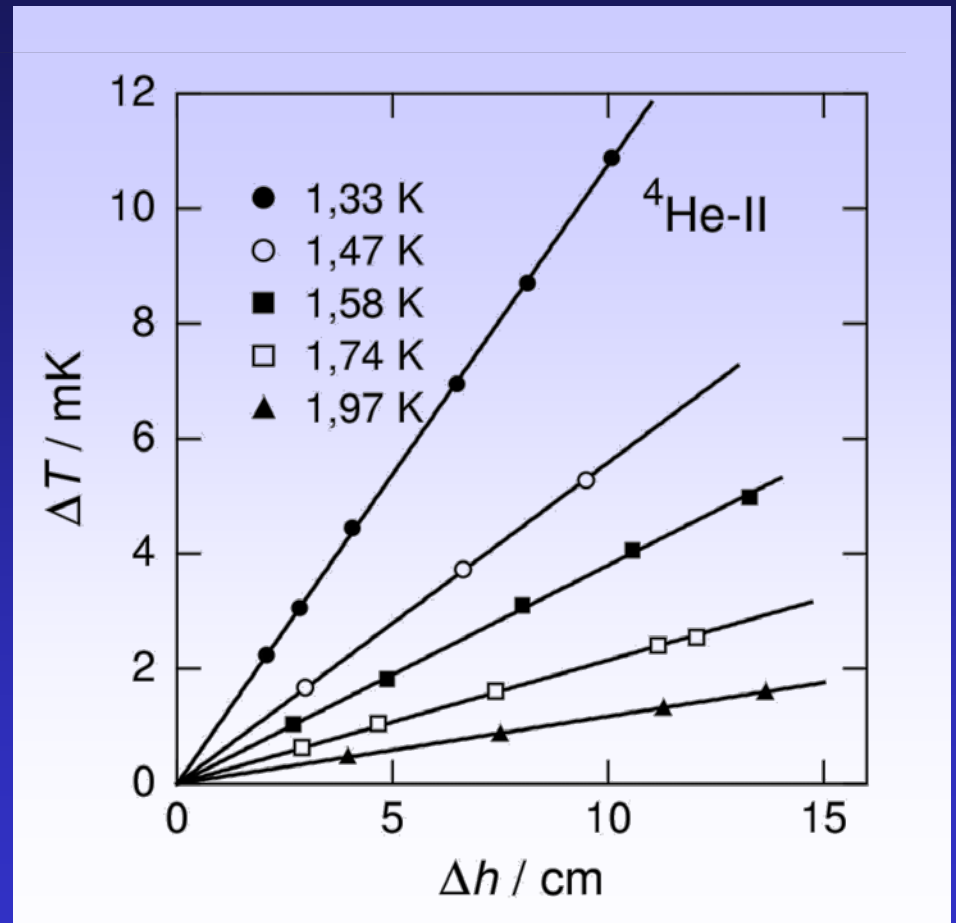
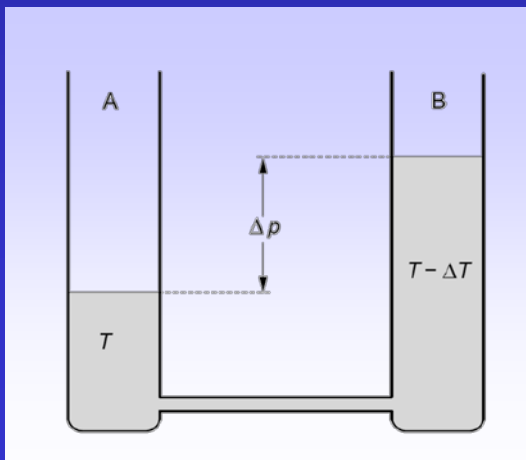
Thermo-mechanical Effect

In equilibrium:

$$\frac{\partial \mathbf{v}_s}{\partial t} = S \operatorname{grad} T - \frac{1}{\varrho} \operatorname{grad} p = 0$$

(H.) London equation:

$$\frac{\Delta p}{\Delta T} = \varrho S$$



Sound Propagation

From two-fluid hydrodynamics:

$$\frac{\partial^2 \varrho}{\partial t^2} = \nabla^2 p \quad \frac{\partial^2 S}{\partial t^2} = \frac{\varrho_s S^2}{\varrho_n} \nabla^2 T$$

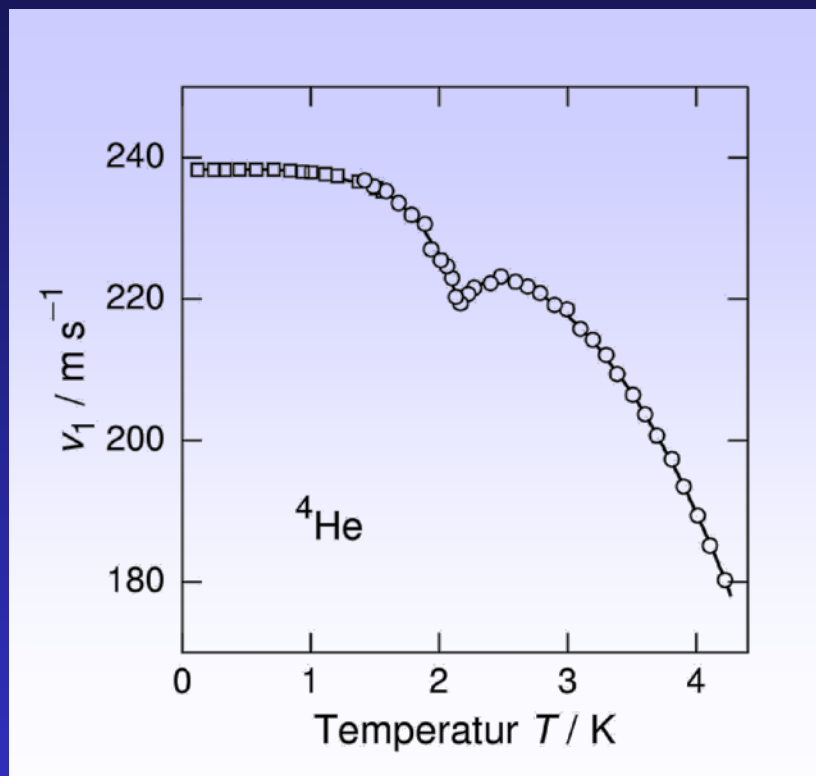
Can be transformed into:

$$\left[\left(\frac{v}{v_1} \right)^2 - 1 \right] \left[\left(\frac{v}{v_2} \right)^2 - 1 \right] = \frac{C_p - C_V}{C_p} \quad \text{two weakly coupled modes}$$

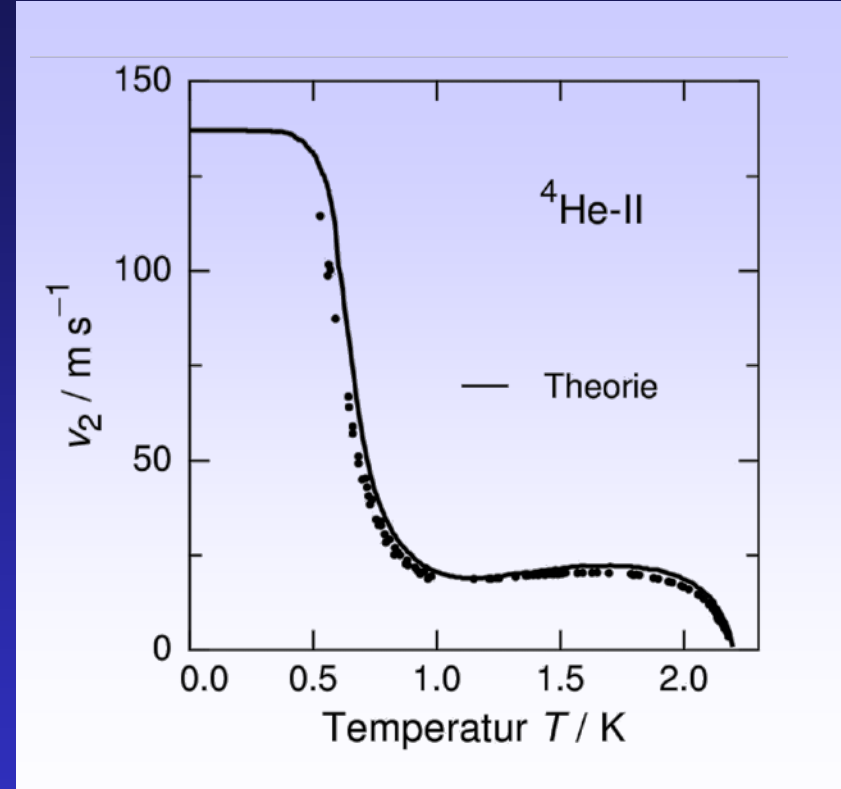
with

$$v_1^2 = \left(\frac{\partial p}{\partial \varrho} \right)_S \quad \text{and} \quad v_2^2 = \frac{\varrho_s}{\varrho_n} S^2 \left(\frac{\partial T}{\partial S} \right)_{\varrho}$$

First Sound



Second Sound

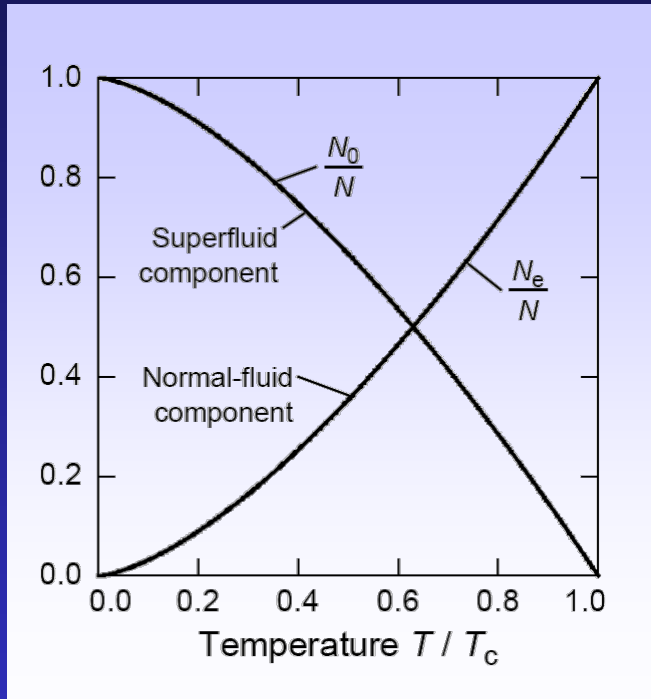


$$\boldsymbol{v}_n = \boldsymbol{v}_s$$

$$\varrho_n \boldsymbol{v}_n + \varrho_s \boldsymbol{v}_s = 0$$

$$T \rightarrow 0 \quad v_2 \rightarrow v_1/\sqrt{3} \simeq 137 \text{ m/s}$$

Bose-Einstein Condensation



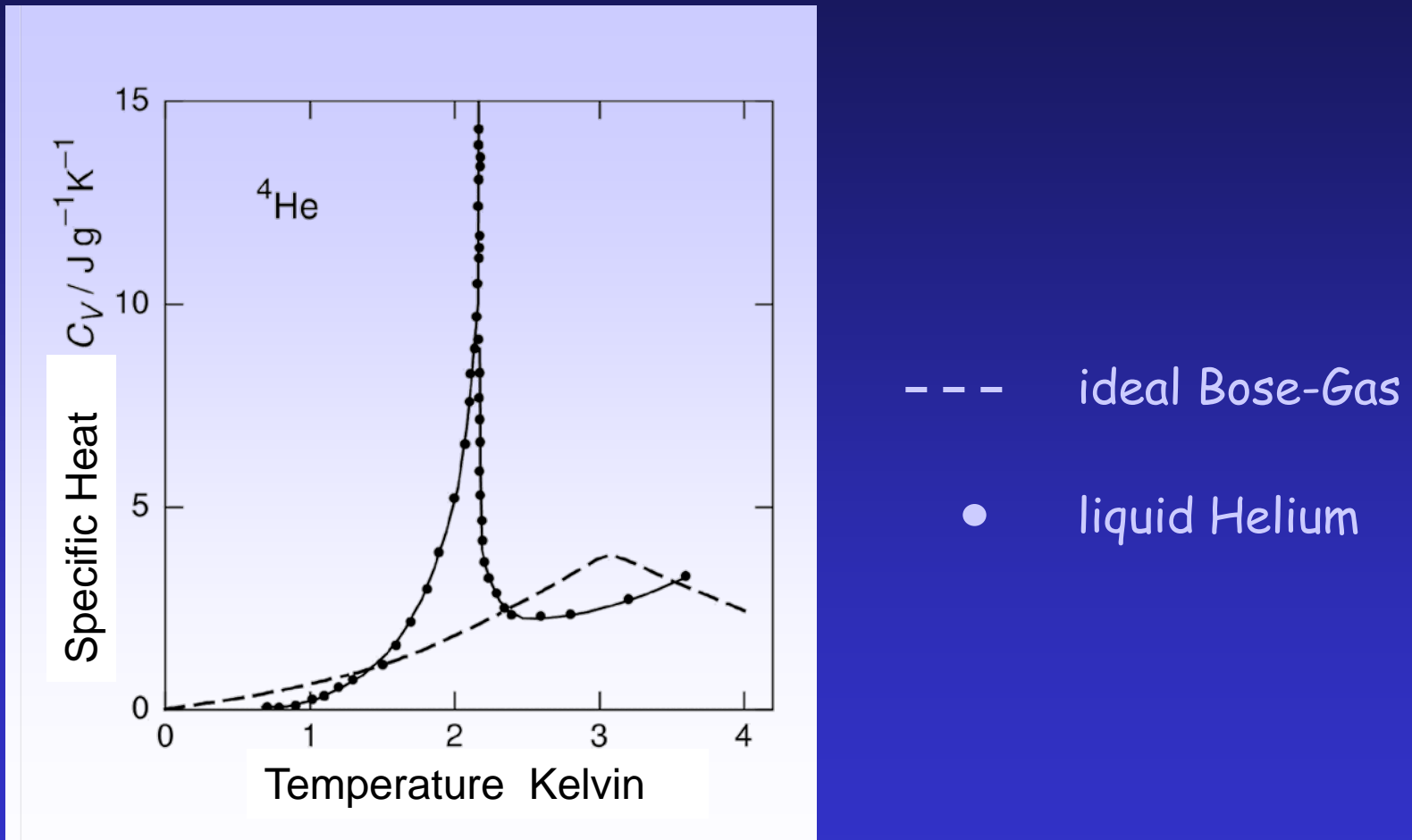
$$N = N_0 + \frac{V}{4\pi^2} \left(\frac{2m}{\hbar^2} \right)^{3/2} \int_0^{\infty} \frac{\sqrt{E}}{e^{(E-\mu)/k_B T} - 1} dE$$

© Université de Montréal

$$N \approx N_0 + 2.6 \frac{V}{V_Q}$$

$$N_e(T_c) = N \text{ and } N_0(T_c) = 0$$
$$\frac{N_e}{N} = \left(\frac{T}{T_c} \right)^{3/2}$$
$$T_c = \frac{2\pi\hbar^2}{k_B m} \left(\frac{N}{2.6V} \right)^{2/3}$$

Specific Heat



Macroscopic Quantum State

Macroscopic wave function

$$\psi(\mathbf{r}) = \psi_0 e^{i\varphi(\mathbf{r})}$$

$$\psi^* \psi = |\psi_0|^2 = \frac{\varrho_s}{m_4}$$

$$-i\hbar \nabla \psi = \mathbf{p} \psi$$

$$\mathbf{p} = \hbar \nabla \varphi(\mathbf{r}) = m_4 \mathbf{v}_s$$

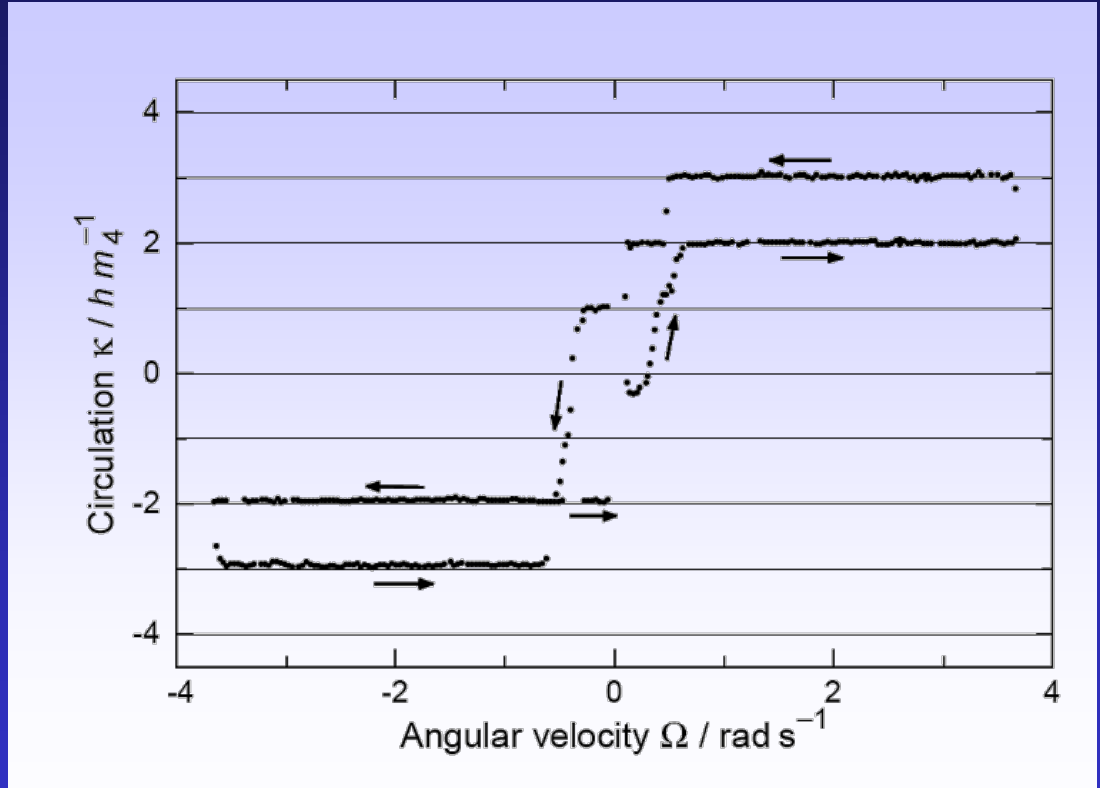
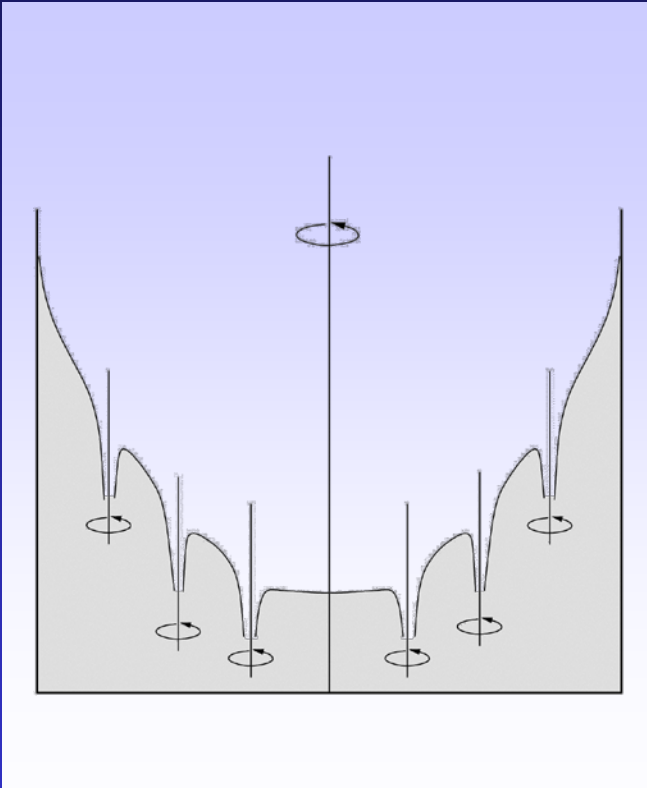
$$\mathbf{v}_s = \frac{\hbar}{m_4} \nabla \varphi(\mathbf{r})$$

$$\kappa = \oint_L \mathbf{v}_s \cdot d\mathbf{l} \quad \Delta\varphi = 2\pi n$$

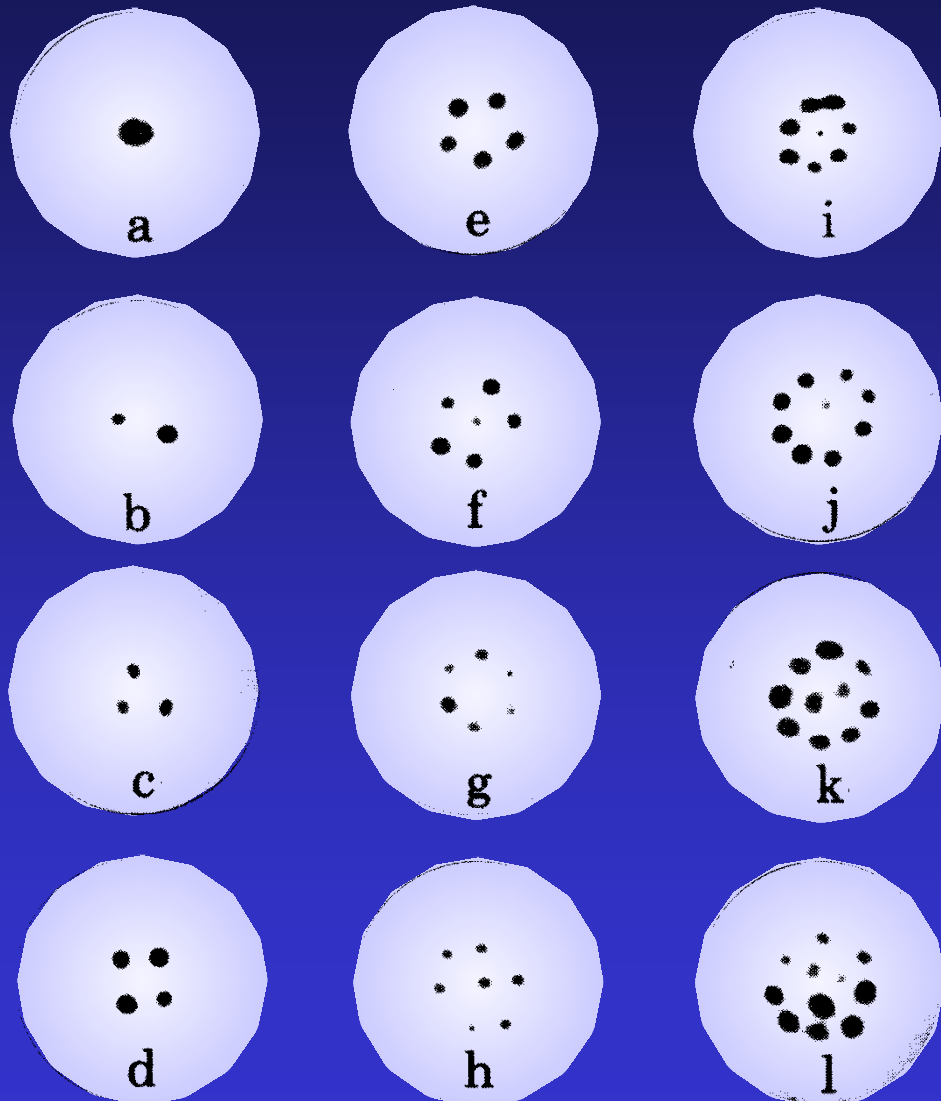
Quantized circulation

$$\kappa = \frac{\hbar}{m_4} n$$

Quantization of Circulation



Vortices with Quantized Circulation



$T = 0,1 \text{ K}$

$d = 2 \text{ mm}$

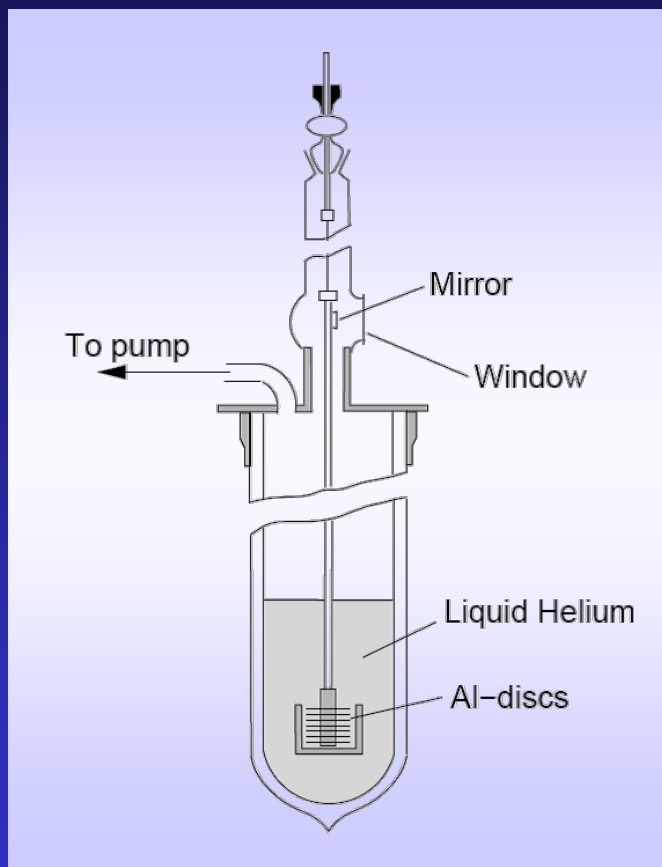
$\ell = 25 \text{ mm}$

(a) \longrightarrow (l)

3 \longrightarrow 8 Rev./min

Determination of ρ_n

Andronikashvili 1948

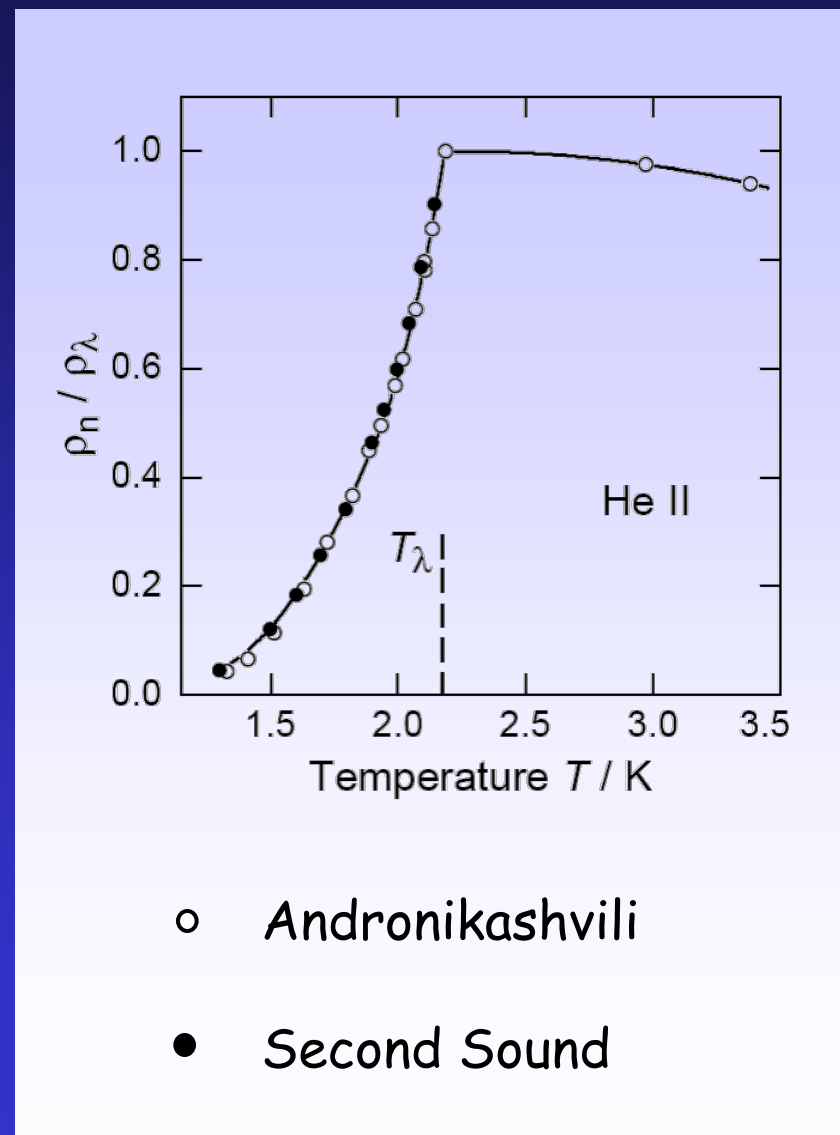


50 Aluminium discs

Thickness 13 μm

Diameter 3,5 cm

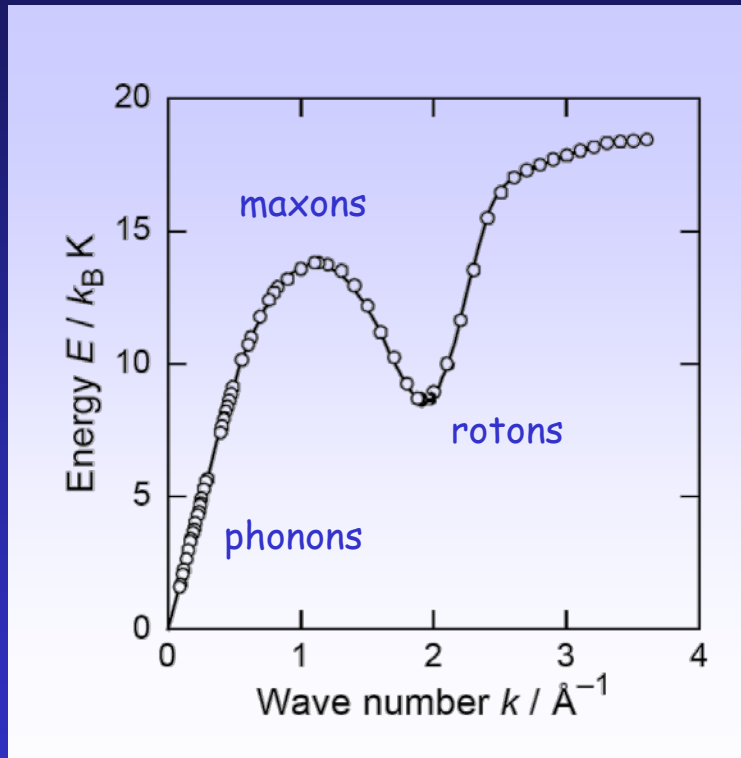
Distance 210 μm



○ Andronikashvili

● Second Sound

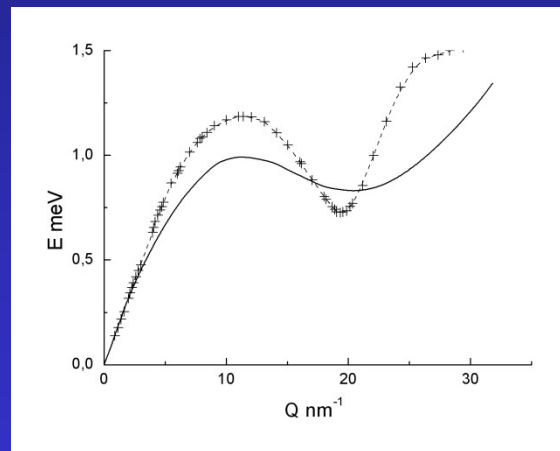
Excitation Spectrum of superfluid ^4He



Well-defined collective excitations

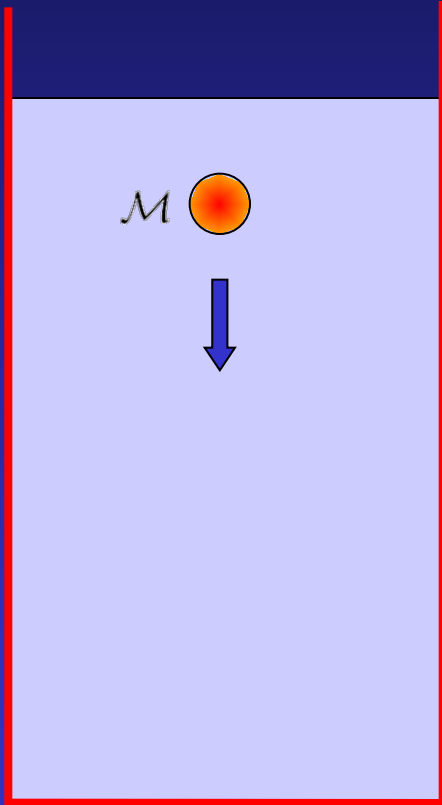
Phonons and Rotons

No single particle excitations



Theory: Landau

Concept of a Critical Velocity



$$T = 0$$

one excitation with: energy \mathcal{E} and momentum p

energy conservation

$$\frac{1}{2}\mathcal{M}v^2 = \frac{1}{2}\mathcal{M}v'^2 + \mathcal{E}$$

momentum conservation

$$\mathcal{M}v - p = \mathcal{M}v'$$

Critical velocity

$$\left. \begin{array}{l} \text{energy conservation} \\ \frac{1}{2}\mathcal{M}v^2 = \frac{1}{2}\mathcal{M}v'^2 + \mathcal{E} \\ \text{momentum conservation} \\ \mathcal{M}v - p = \mathcal{M}v' \end{array} \right\} v \cdot p - \frac{1}{2\mathcal{M}} p^2 = \mathcal{E}$$

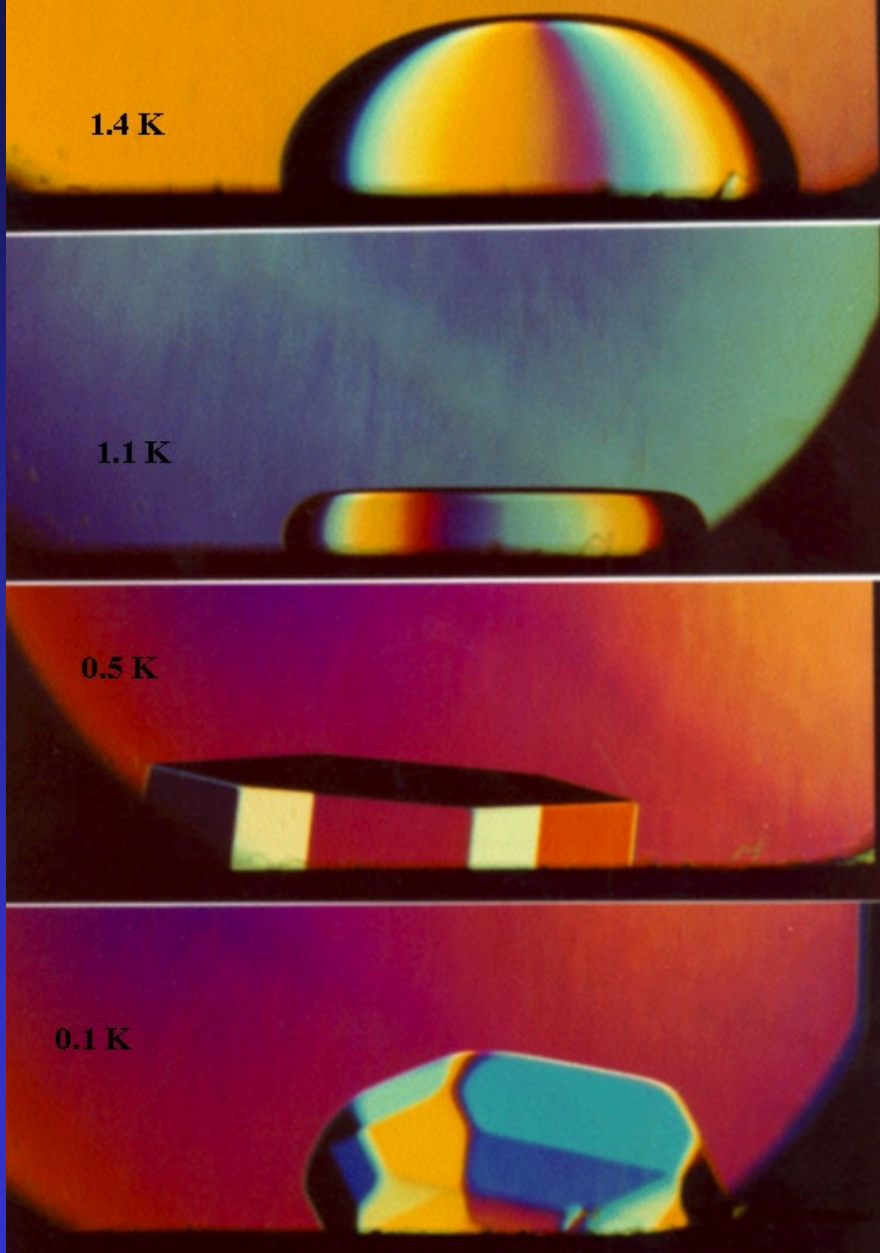
$$v_c = \frac{\mathcal{E}}{p}$$

Solid ${}^4\text{He}$



S.BALIBAR, C.GUTHMANN nad E.ROLLEY (ENS PARIS)

THE ROUGHENING TRANSITIONS
OF HELIUM 4 CRYSTALS

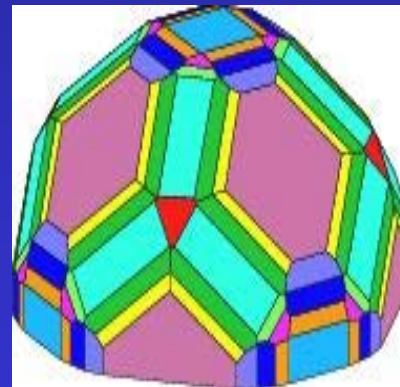
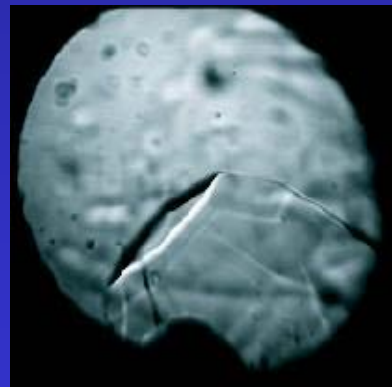


Crystallization waves in helium-4.



Photograph taken by S. Balibar, C. Guthmann and E. Rolley in Paris.

Growing helium-3 crystal at 2.2 mK



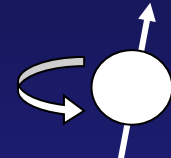
Eleven different types of facets observed on the surface of helium-3 crystals.

from Wagner *et al.*, Phys Rev. Lett. **76**, 263 (1996).

Nuclear magnetism of ^3He

^3He atom : nuclear spin $\frac{1}{2}$

Fermion!



Nuclear magnetic moment : $\mu = -2.1274 \mu_\text{n}$

$\mu/k_B = 7.78255 \cdot 10^{-4} \text{ Kelvin/Tesla}$

$\gamma/2\pi = 32.435 \text{ MHz/Tesla}$

Spin $\frac{1}{2}$, large magnetic moment, good nucleus for NMR!!!

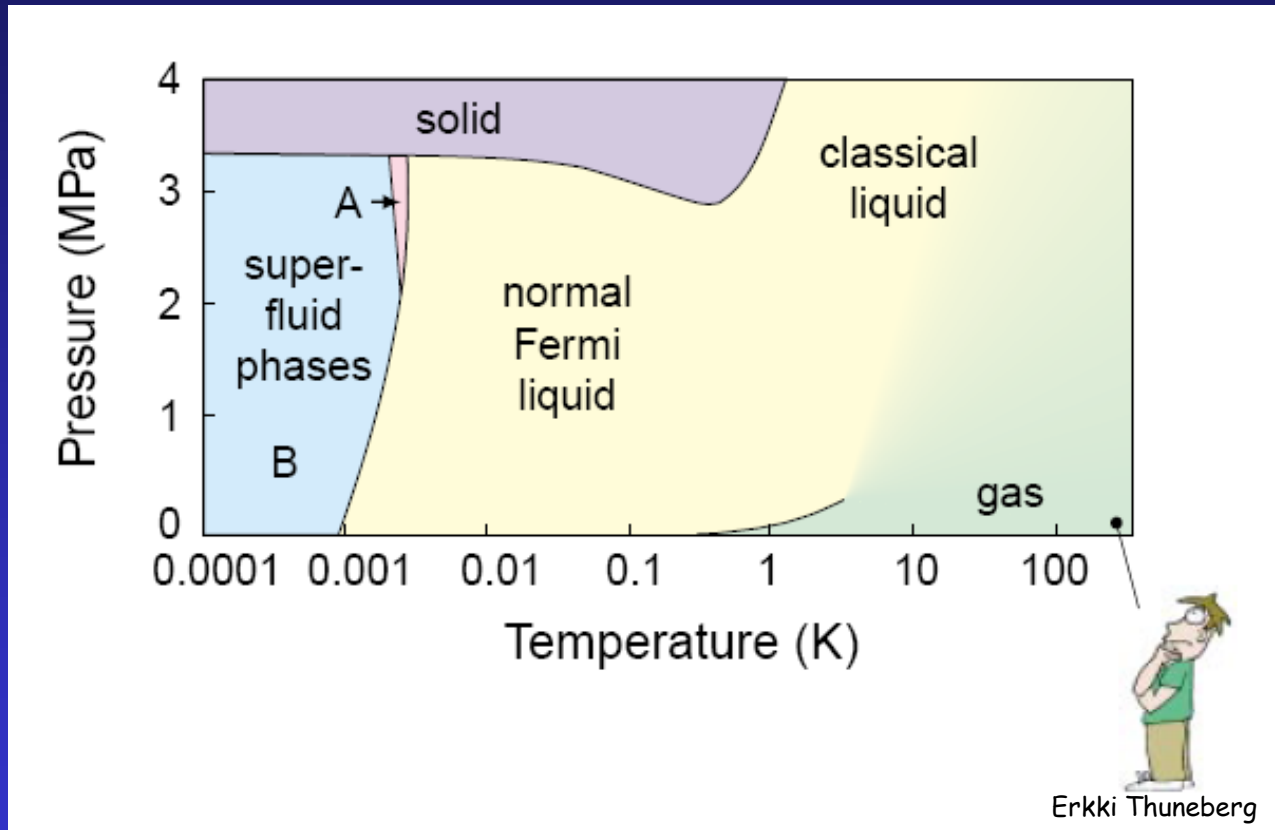
In the solid phases the atoms are quasi-localized

Zero point energy is comparable to the potential well depth, about 10 K (structural energies!).

Large tunneling of atoms (frequency of order MHz)
Quantum exchange interactions : $J \sim 1 \text{ mK}$.

Small dipole-dipole interactions $E_D \sim \mu^2/a^3 \sim \mu\text{K}$

Phase Diagram of ${}^3\text{He}$



Melting curve

$T > 1 \text{ K}$: classical phase diagram

$T < 1 \text{ K}$: the entropy of the solid is larger than that of the liquid

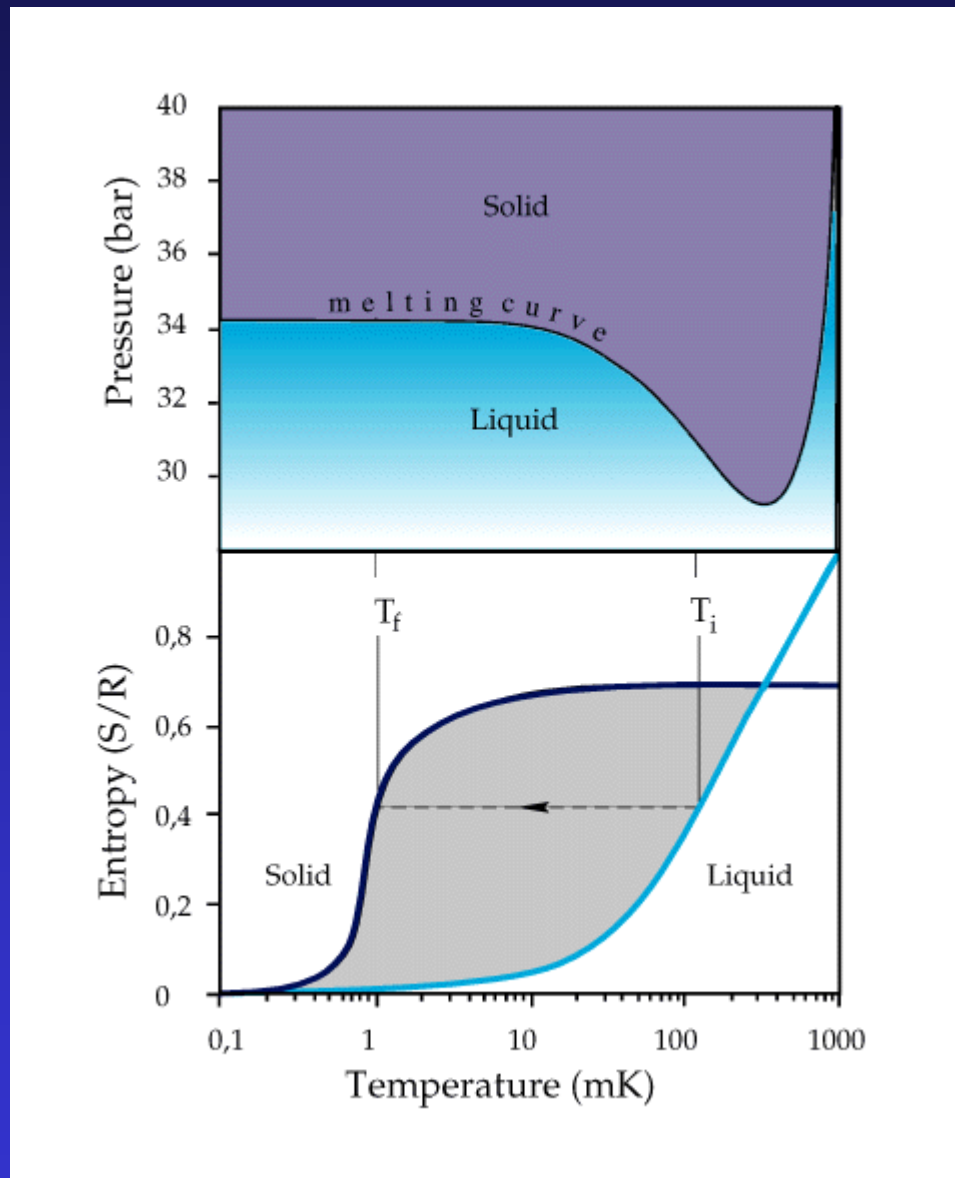
Disordered solid (spin entropy)

Liquid is ordered in k-space (FermiLiquid)

→ Minimum of the melting curve

(Clausius-ClapeyronEquation)

Solid nuclear order at $T \sim 1 \text{ mK}$



Landau theory of Fermi liquids

$$C = \gamma T \quad (T \ll T_F)$$

$$\chi = C/T_F^{**}$$

$$\eta \propto T^{-2}$$

$$\kappa \propto T^{-1}$$

« Fermi Gas » with renormalised parameters

Theory is subtle!

See Pines and Nozières books

Effective mass m^*

$$C/C_{id} = m^*/m \quad 2,8 \text{ to } 5,8$$

increases with pressure

$$\text{Reinforced magnetism} \quad 9,2 \text{ to } 23,7$$

increases with pressure

$$\frac{C_v}{C_v^{id}} = \frac{m^*}{m} = 1 + \frac{1}{3} F_1^s$$

$$\frac{\chi(0)}{\chi^0(0)} = \frac{m^*}{m} \cdot \frac{1}{1 + F_0^a}$$

Heat Capacity

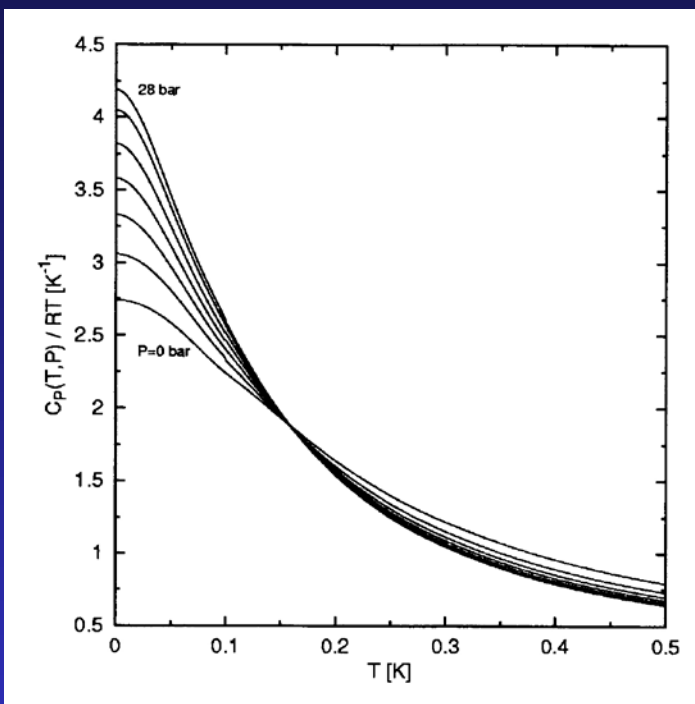


FIG. 5. Specific heat at constant pressure $C_P(T,P)$ divided by temperature vs T at pressures $P=0, 5, 10, 15, 20, 25, 28$ bar. The small kinks at the temperature $T_0=0.1$ K in this and other figures are artefacts caused by the different interpolation formulas (Ref. 16) for $C_V(T,V)$ used below and above T_0 .

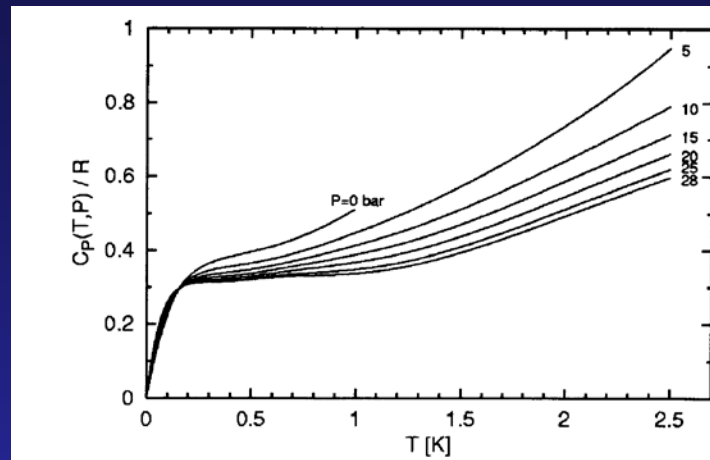


FIG. 6. High-temperature behavior of the specific heat at constant pressure $C_P(T,P)$.

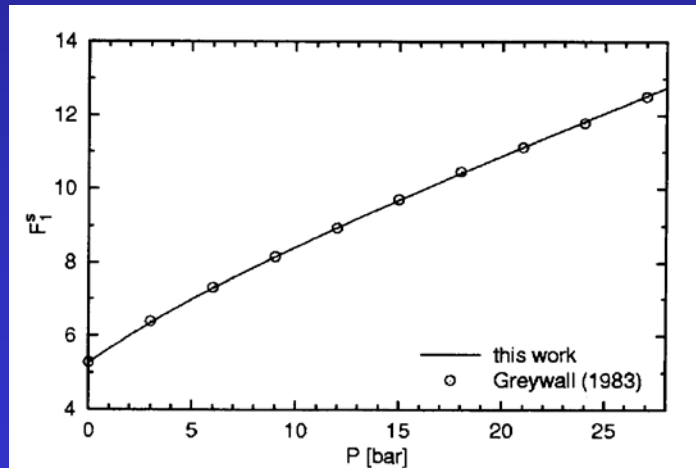
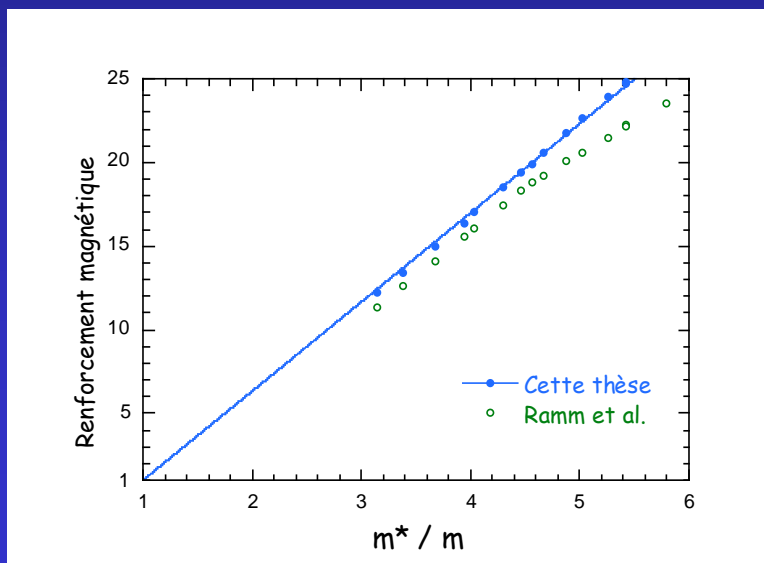
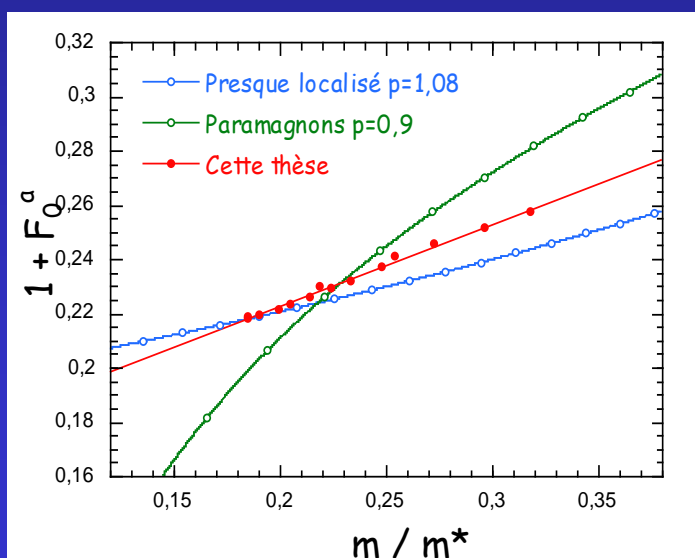
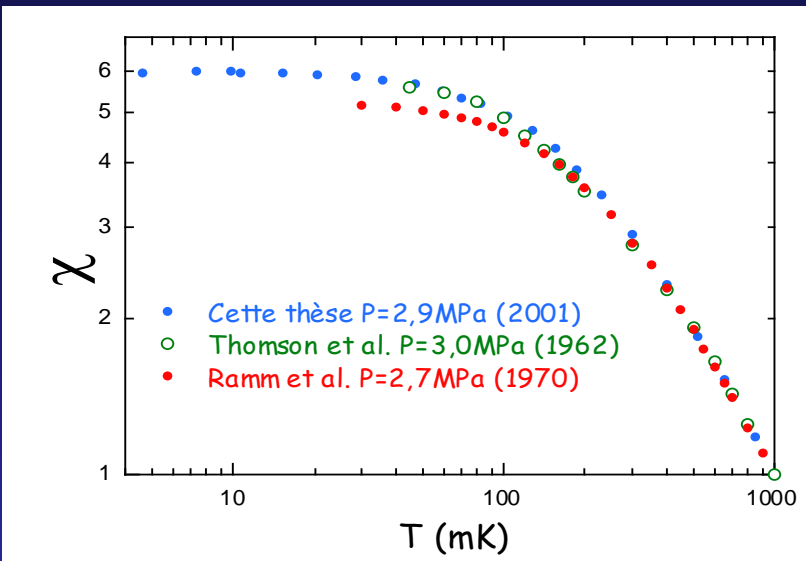
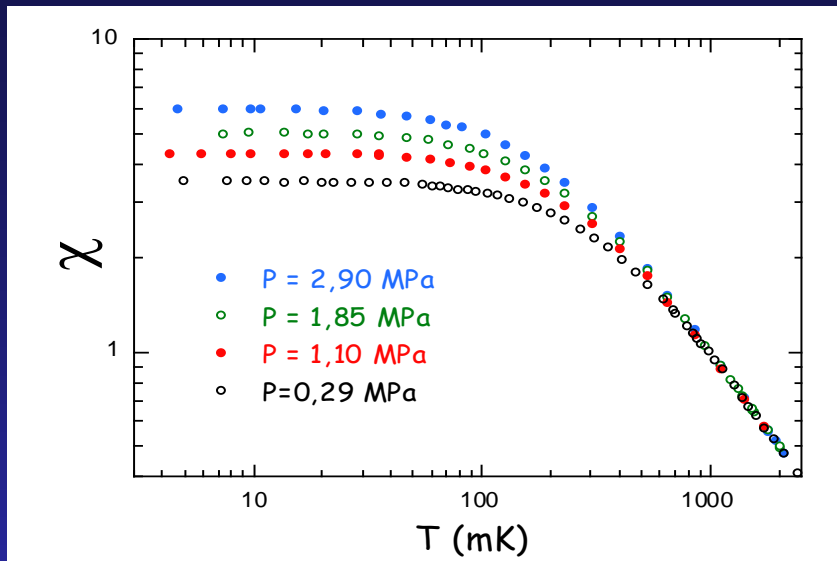


FIG. 9. Fermi-liquid parameter F_1^s vs P , compared to the data obtained by Greywall (Ref. 16).

D.S. Greywall (1983)

Magnetic susceptibility

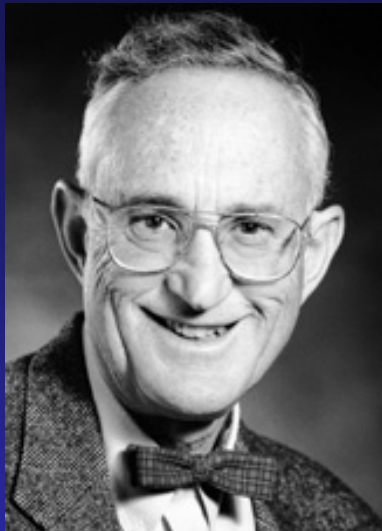


(PhD thesis S. Triqueneaux, 2001; V. Goudon, 2006)

Chichilianne 2011

The Nobel Prize in Physics 1996

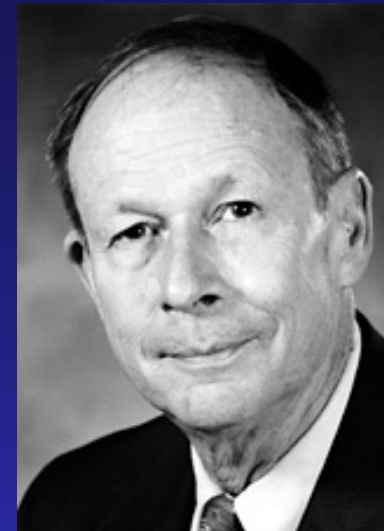
"for their discovery of superfluidity in helium-3"



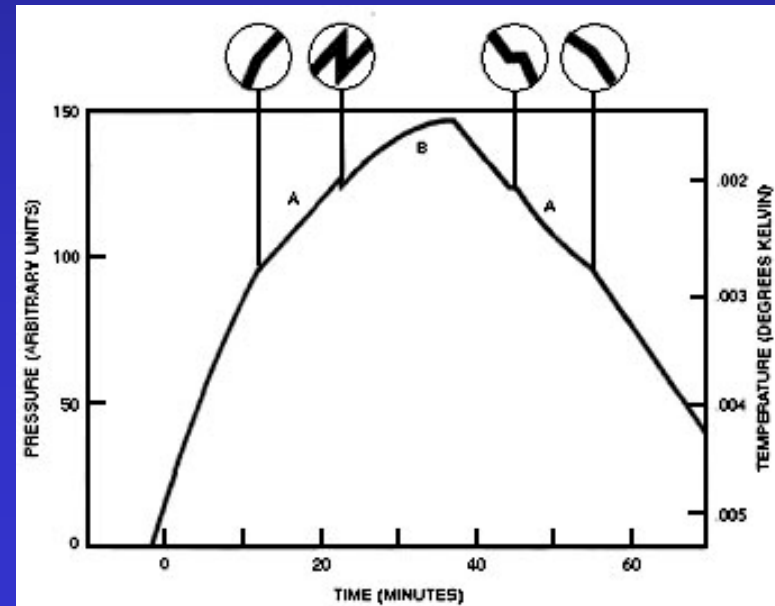
David M. Lee



Douglas D. Osheroff

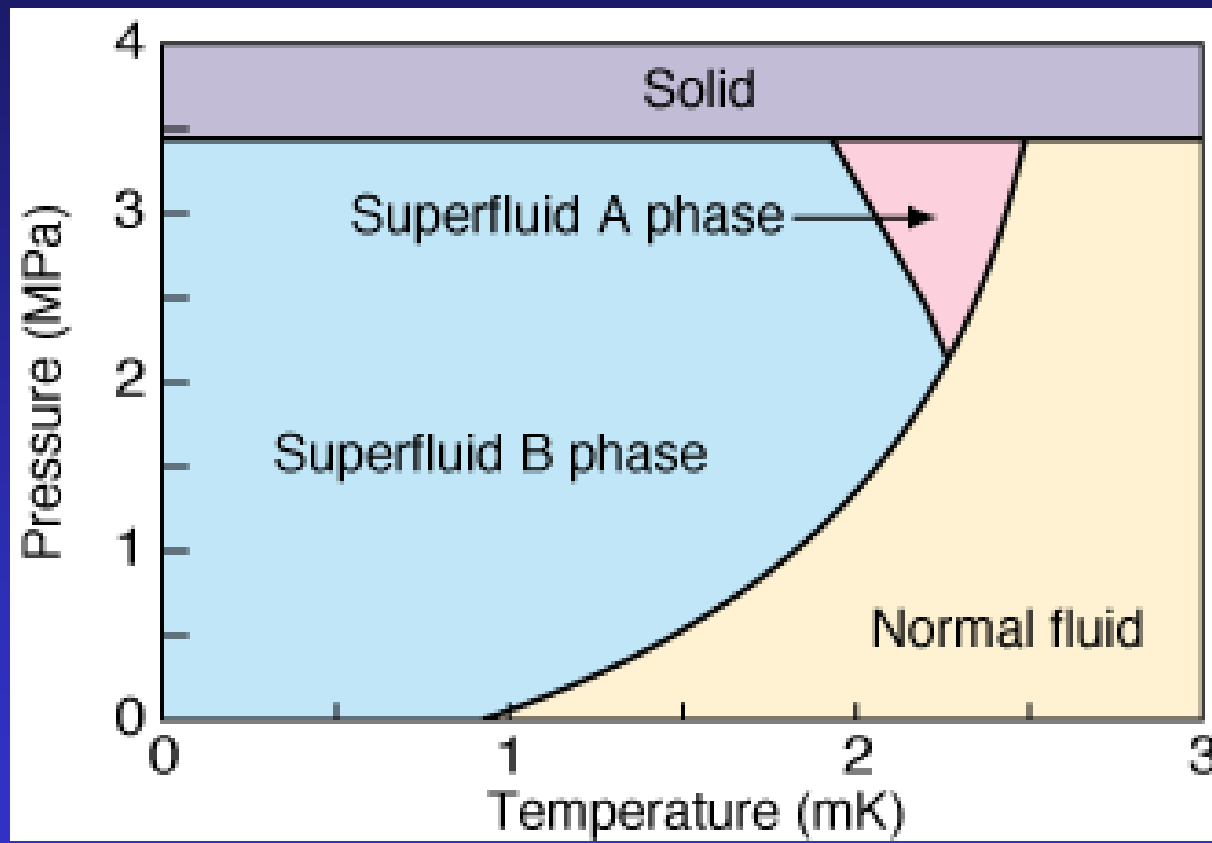


Robert C. Richardson



The figure shows the pressure inside a sample containing a mixture of liquid helium-3 and solid helium-3 ice. The sample is first subjected to increasing external pressure for about 40 minutes, whereafter the external pressure is reduced. Note the changes in the slope of the curve at A and B and the temperatures at which these occur. The graph resembles that published by D.D. Osheroff, R.C. Richardson and D.M. Lee in Physical Review Letters 28, 885 (1972) in which the new helium-3 phase transitions were first reported.

Low temperature phase diagram



Cooper pairs in superfluid ^3He

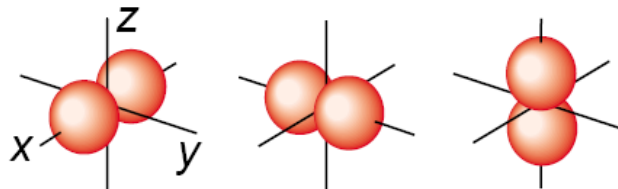
Spin wave functions ($S=1$)

$$S_x=0: (-\uparrow\uparrow + \downarrow\downarrow)$$

$$S_y=0: i(\uparrow\uparrow + \downarrow\downarrow)$$

$$S_z=0: (\uparrow\downarrow + \downarrow\uparrow)$$

Orbital wave functions ($L=1$)

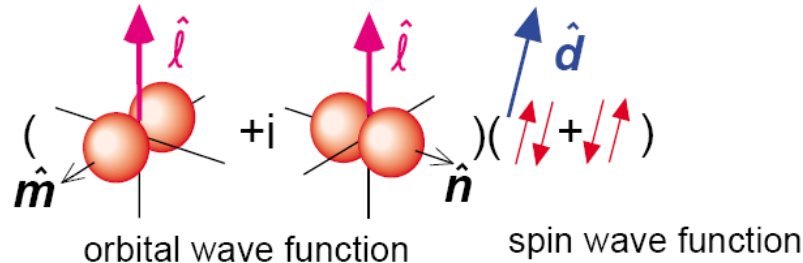


$$\begin{pmatrix} A_{xx} & A_{xy} & A_{xz} \\ A_{yx} & A_{yy} & A_{yz} \\ A_{zx} & A_{zy} & A_{zz} \end{pmatrix}$$

order parameter

The A phase

The order parameter $A_{\mu j} = \Delta \hat{d}_{\mu} (\hat{m}_j + i \hat{n}_j)$



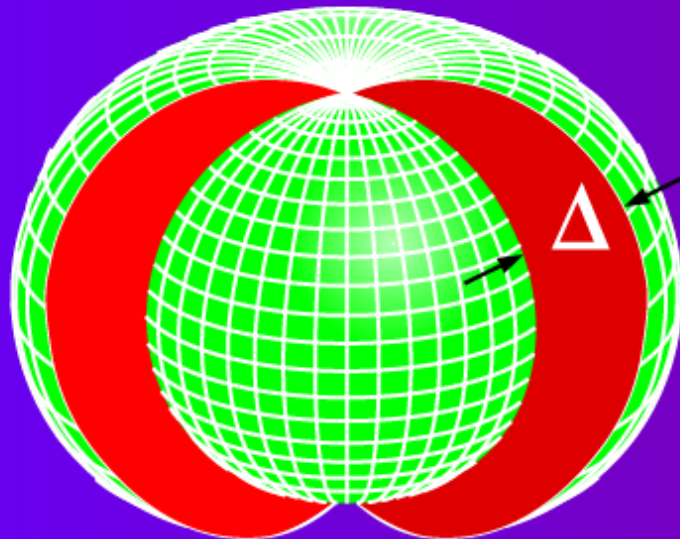
A phase factor $e^{i\chi}$ corresponds to rotation of \hat{m} and \hat{n} around \hat{l} :

$$\begin{aligned} e^{i\chi}(\hat{m} + i\hat{n}) &= (\cos \chi + i \sin \chi)(\hat{m} + i\hat{n}) \\ &= (\hat{m} \cos \chi - \hat{n} \sin \chi) + i(\hat{m} \sin \chi + \hat{n} \cos \chi). \end{aligned}$$

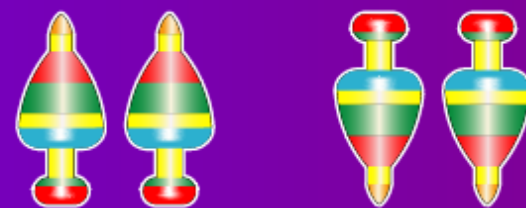
Superfluid velocity

$$\mathbf{v}_s = \frac{\hbar}{2m} \nabla \chi = \frac{\hbar}{2m} \sum_j \hat{m}_j \nabla \hat{n}_j.$$

A-phase: $A_{\mu i} = \Delta e^{i\varphi} d_\mu (m_i + i n_i)$



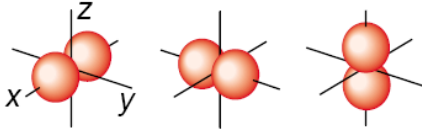
A-phase gap



A-phase has only spin $\uparrow\uparrow$ pairs
and spin $\downarrow\downarrow$ pairs

Superfluid B phase

Orbital wave functions ($L=1$)



Spin wave functions ($S=1$)

$S_x=0$: $(-\uparrow\uparrow + \downarrow\downarrow)$

$S_y=0$: $i(\uparrow\uparrow + \downarrow\downarrow)$

$S_z=0$: $(\uparrow\downarrow + \downarrow\uparrow)$

$$\begin{pmatrix} A_{xx} & A_{xy} & A_{xz} \\ A_{yx} & A_{yy} & A_{yz} \\ A_{zx} & A_{zy} & A_{zz} \end{pmatrix} = A_0 e^{i\phi} \begin{pmatrix} R_{xx} & R_{xy} & R_{xz} \\ R_{yx} & R_{yy} & R_{yz} \\ R_{zx} & R_{zy} & R_{zz} \end{pmatrix}$$

order parameter

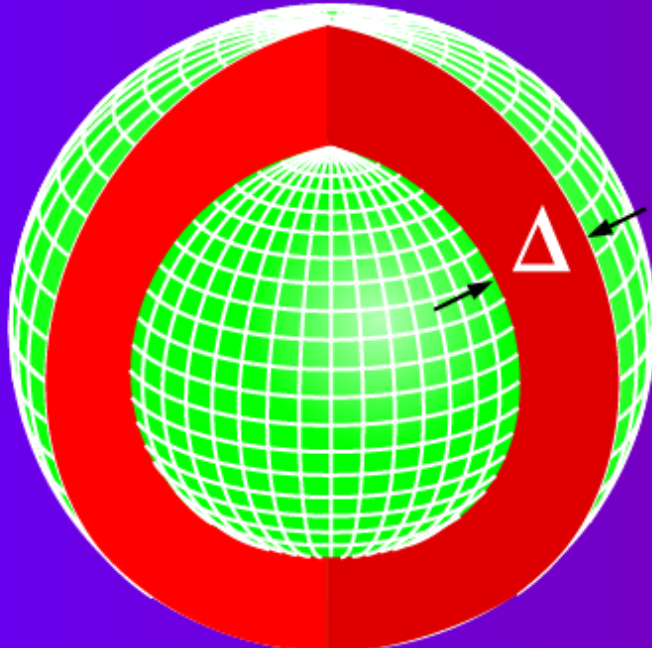
amplitude (real)

phase factor (complex)

rotation matrix (real)

$\begin{cases} \text{angle } \theta = 104^\circ \\ \text{axis } \mathbf{n} \end{cases}$

B-phase: $A_{\mu i} = |\Delta| e^{i\varphi} \mathbf{R}(\hat{\mathbf{n}}, \theta)_{\mu i}$ $\mu, i = 1, 2, 3$



B-phase gap



B-phase has all three components;
spin $\uparrow\uparrow$ pairs, spin $\downarrow\downarrow$ pairs
and spin $\downarrow\uparrow$ pairs

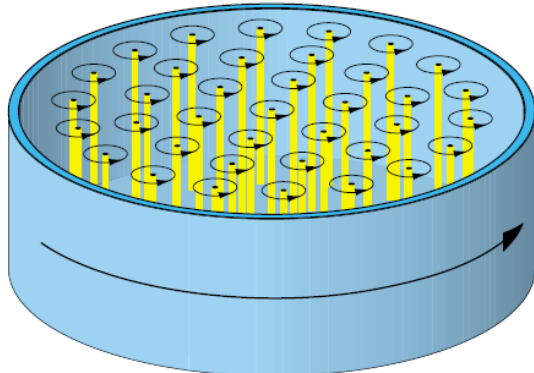
Rotation and vortices

Problem of a rotating superfluid

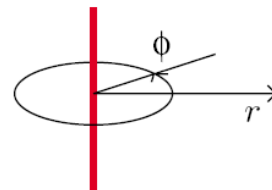
An uncharged superfluid cannot rotate homogeneously:

$$\begin{aligned} A(\mathbf{r}) &= A_0 \exp[i\chi(\mathbf{r})] \\ \Rightarrow \mathbf{v} &= \frac{\mathbf{p}}{2m} = \frac{-i\hbar\nabla}{2m} = \frac{\hbar}{2m}\nabla\chi \\ \Rightarrow \nabla \times \mathbf{v} &= 0. \end{aligned}$$

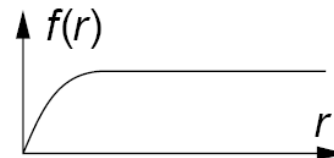
Rotation takes place via vortex lines



Simple model for a vortex



$$A(r, \phi) = A_0 e^{i\phi} f(r)$$



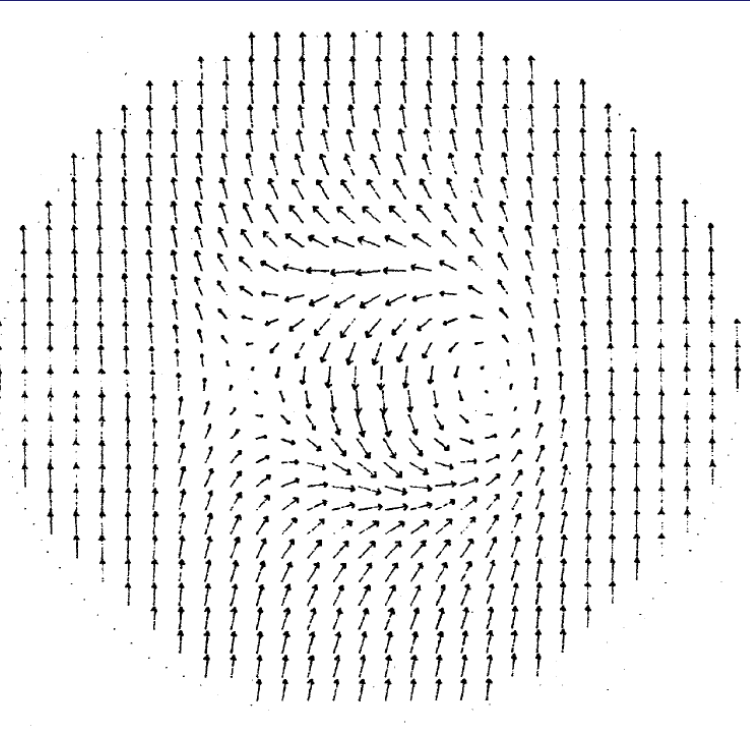
It follows that

$$\mathbf{v} = \frac{\hbar}{2m} \nabla \phi = \frac{\hbar}{2m} \frac{\hat{\phi}}{r}.$$

Circulation around a vortex line

$$\kappa = \oint d\mathbf{l} \cdot \mathbf{v} = \frac{\hbar}{2m} \oint d\mathbf{l} \cdot \nabla \phi = \frac{\hbar}{2m}.$$

Vortex in A phase



Vortex in B phase

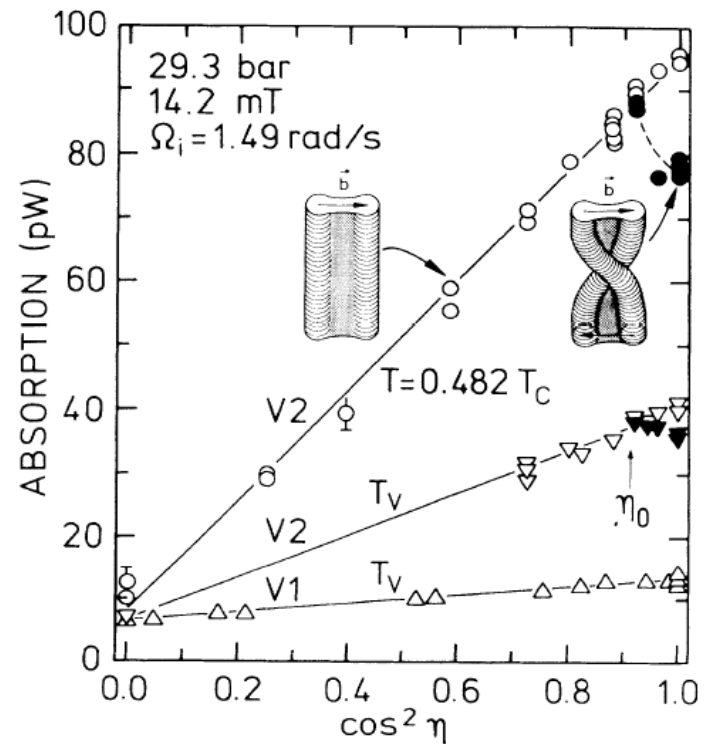
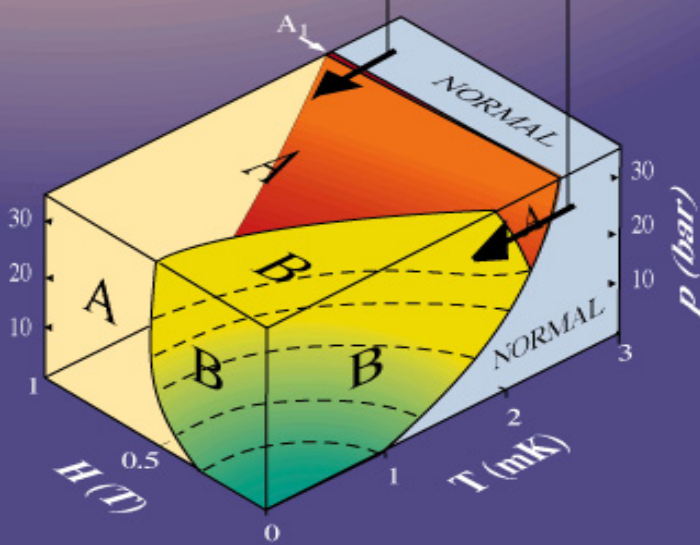
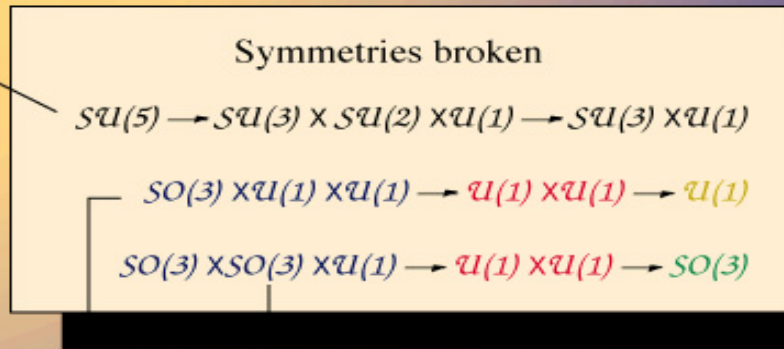


FIG. 2. HPD absorption of an isolated vortex cluster vs the orientation of the applied magnetic field: \circ , V_2 vortex in the untwisted state at $0.48T_c$ with $a_2/a_0 \approx 10.5$ [cf. Eq. (1)] and, \bullet , in the twisted state; ∇ , V_2 vortex untwisted at T_V with $a_2/a_0 \approx 4.87$ and, \blacktriangledown , twisted; \triangle , V_1 vortex with $a_2/a_0 \approx 1.02$.

Big Bang



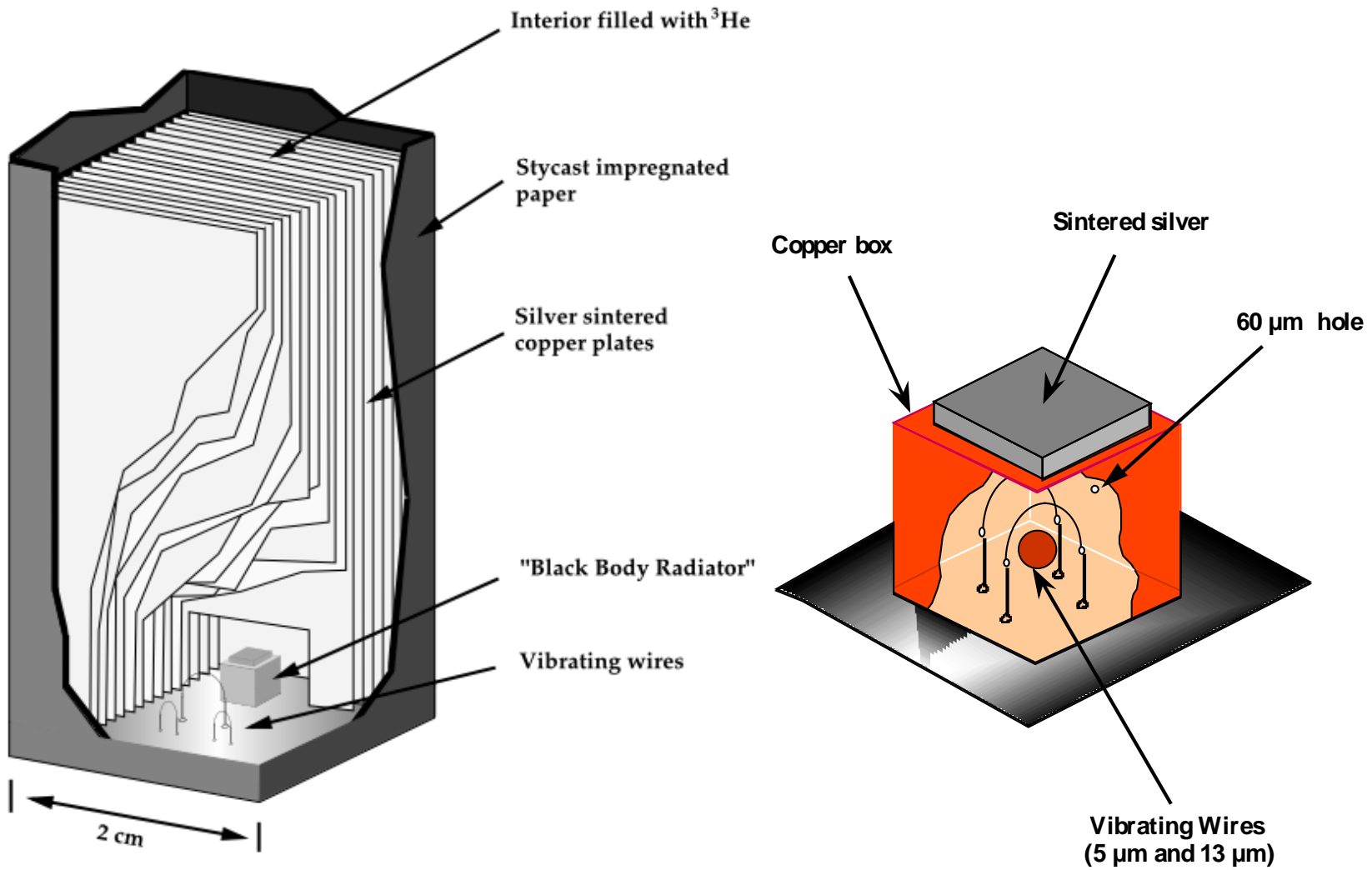
Superfluid ^3He

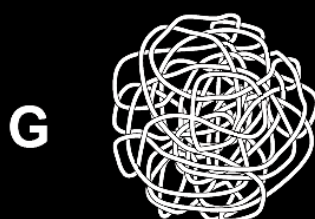
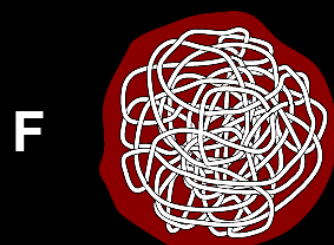
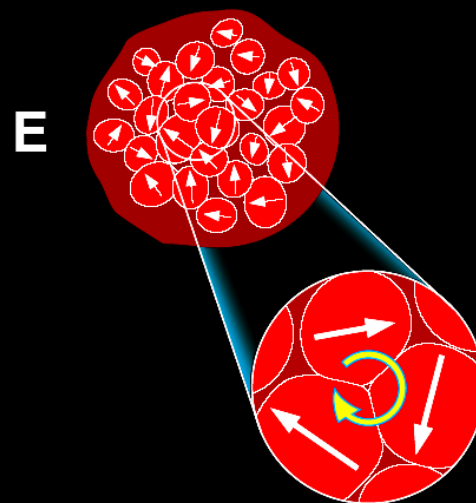
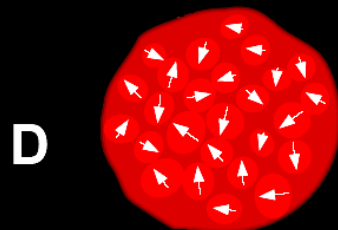
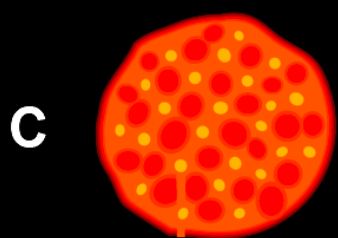
$$\psi = \sqrt{\rho_s} [S] [L] e^{i\varphi}$$

Spin part *Orbital part* *'Gauge' part*

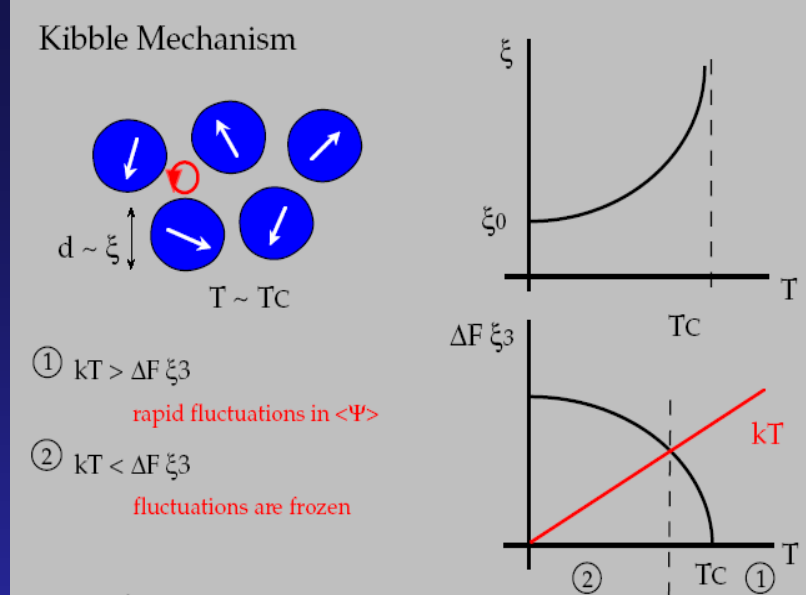
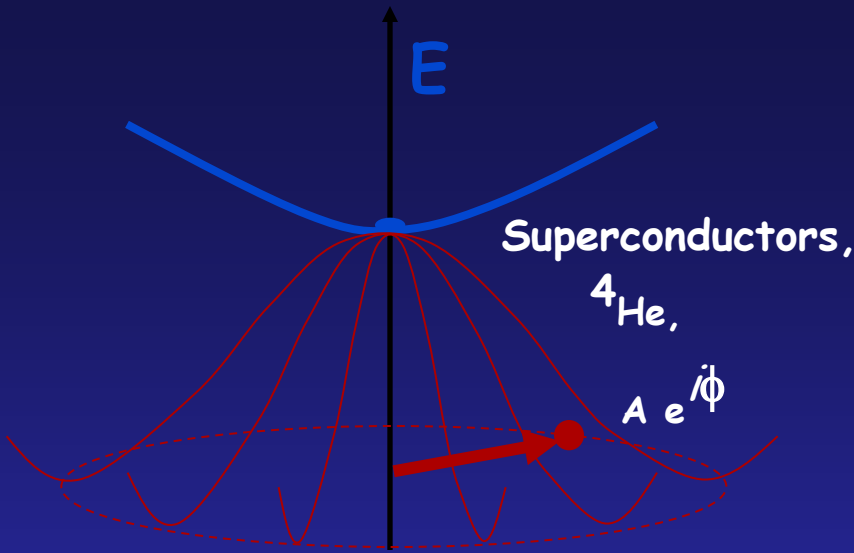
$$SO(3)^S \times SO(3)^L \times U(1)$$

Superfluid ${}^3\text{He}$ bolometry





Topological defects creation and fast transition:



T. W. B. Kibble, J. Phys. A **9**, 1387 (1976).
W. H. Zurek, Nature (London) **317**, 505 (1985).

Zurek Scenario

domain size is determined by "critical slowing down"

$$\varepsilon = 1 - T/T_c = t/\tau_Q$$

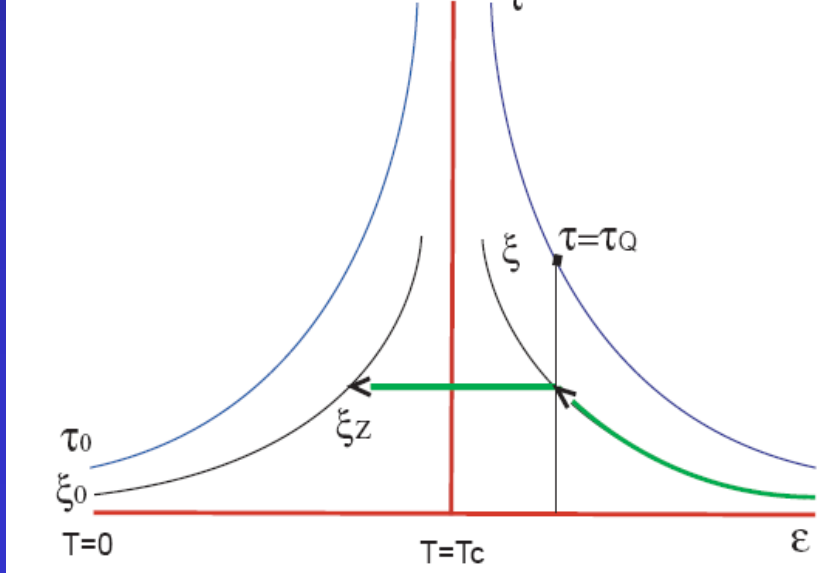
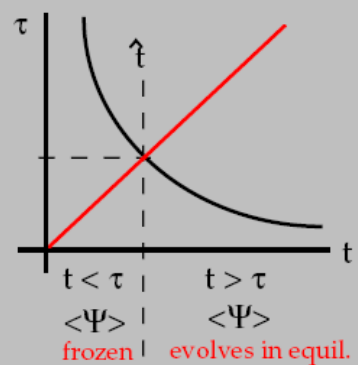
$$\text{corr. length: } \xi = \xi_0 |\varepsilon|^{-1/2}$$

$$\text{char. speed: } v = v_0 |\varepsilon|^{1/2}$$

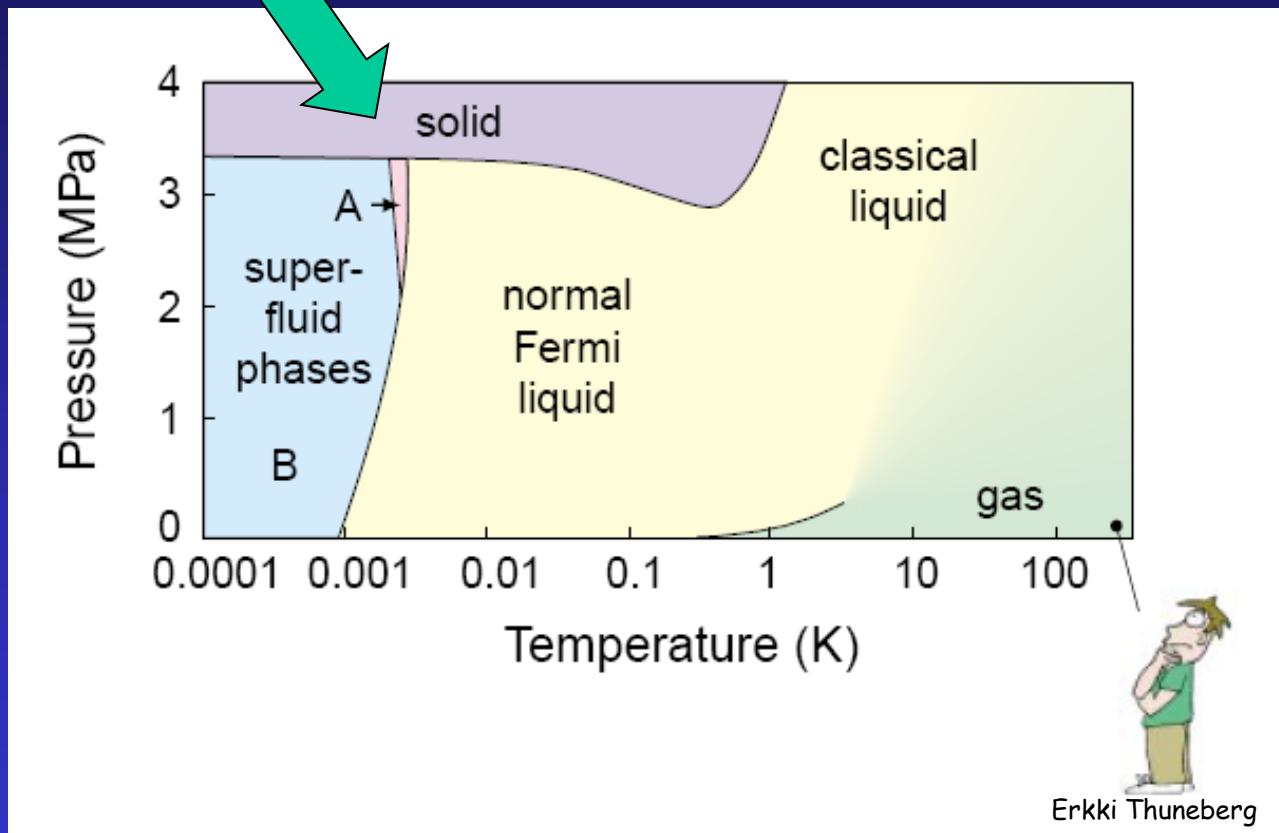
$$\text{corr. time: } \tau = \xi/v = \tau_0 \tau_Q / t$$

$$\text{for } \hat{t} = \tau(\hat{t}) \rightarrow \hat{t} = (\tau_0 \tau_Q)^{1/2}$$

$$d \approx \xi(\hat{t}) = \xi_0 \left(\frac{\hat{t}}{\tau_Q} \right)^{-1/2} = \xi_0 \left(\frac{\tau_Q}{\tau_0} \right)^{1/4} \text{ domain size}$$



Phase Diagram of ${}^3\text{He}$



Multi-spin exchange: of quasi-localized Fermions

- Identical particles
- Hamiltonian without explicit spin-dependent interactions

Pauli principle: the spin state is coupled to the parity of the wave function

Permutation of spins & particles: Dirac (1947) : Effective Hamiltonian on spin variables

$$H_{ex} = -\sum P (-1)^P J_P P$$

Two-particle permutations: $P_2 = (1 + \sigma_i \cdot \sigma_j)$ (Heisenberg Hamiltonian)

Multi-spin exchange in solid ^3He (Thouless, 1965)

Three-particle exchange is also Heisenberg

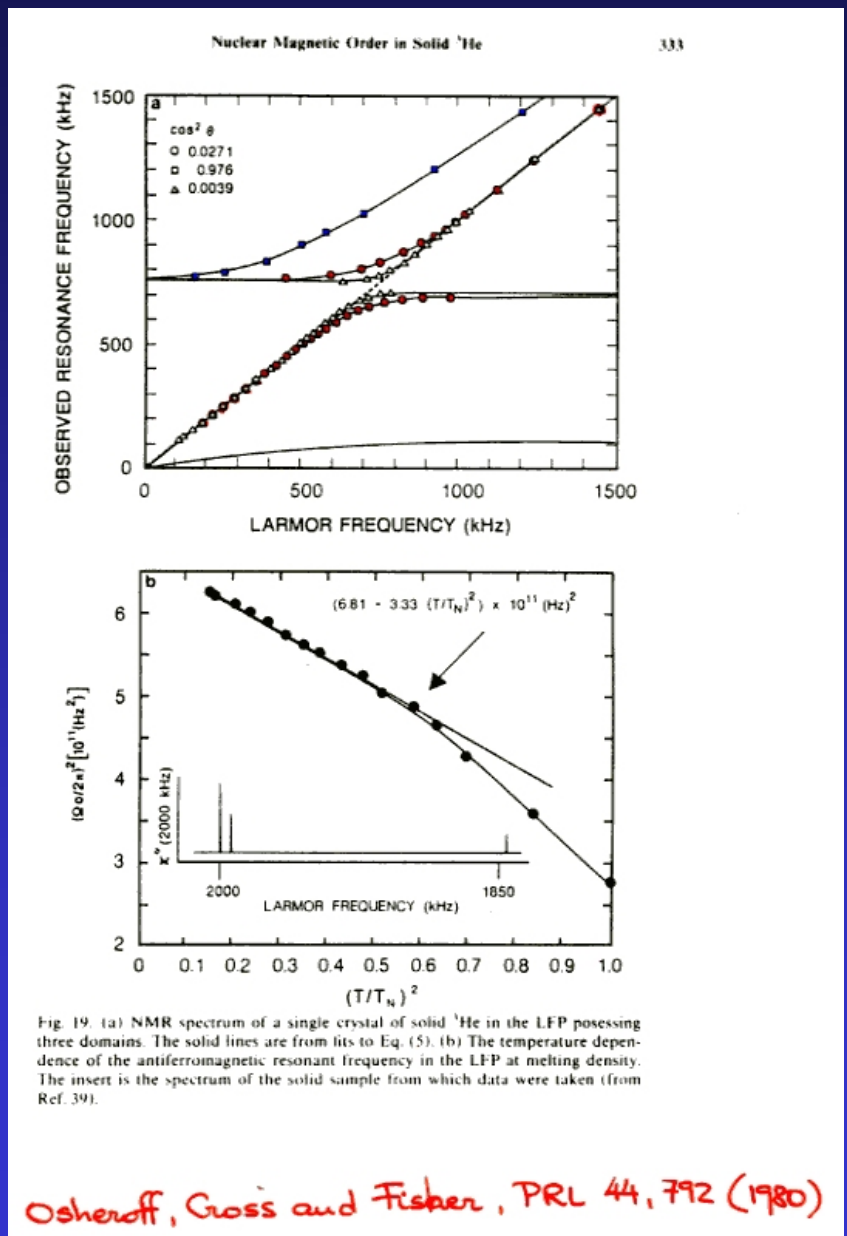
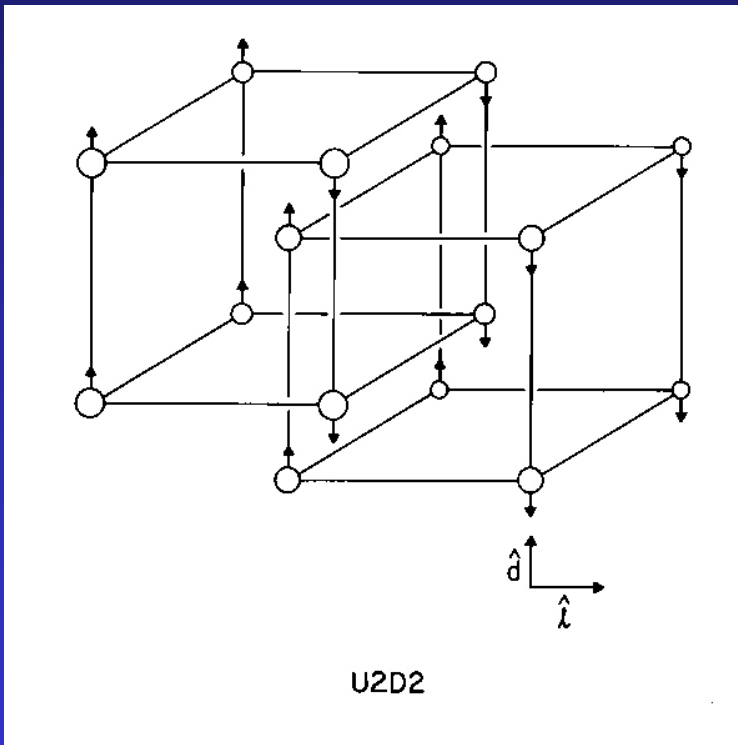
$$P_3 = (1 + \sigma_i \cdot \sigma_j + \sigma_j \cdot \sigma_k + \sigma_k \cdot \sigma_i)$$

Four-spin exchange introduces new physics:

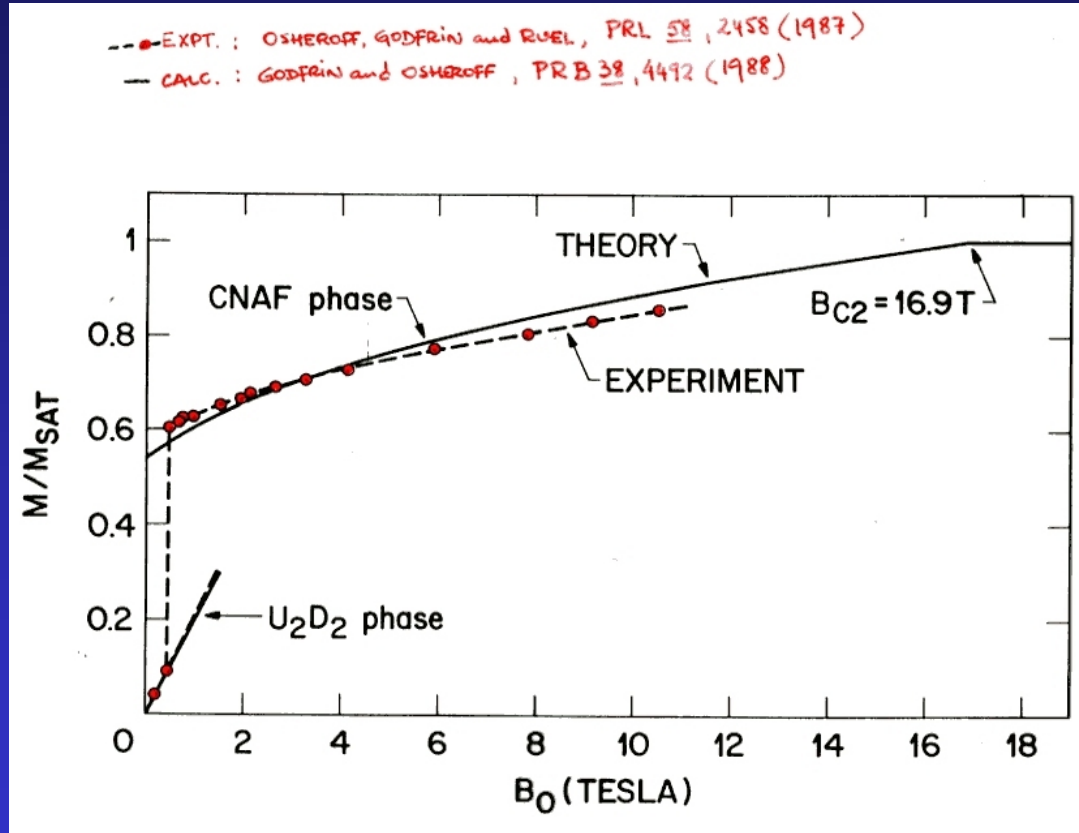
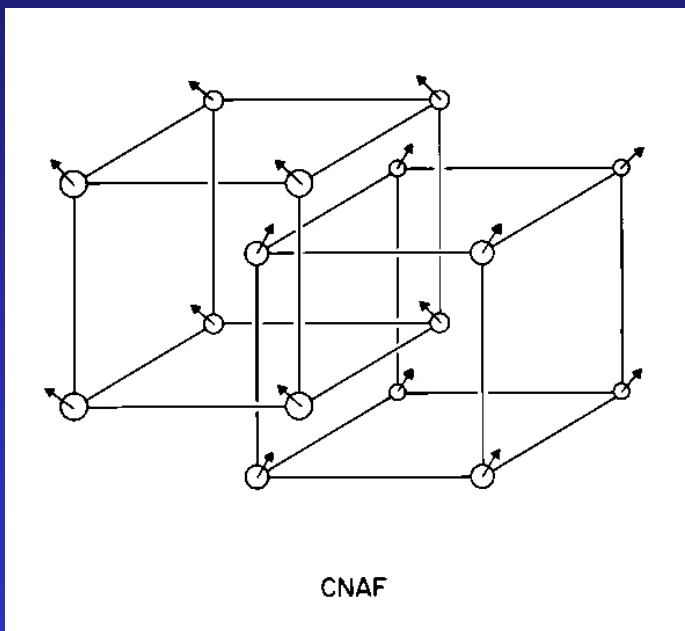
$$P_4 = (1 + \sum \sigma_\mu \cdot \sigma_\nu + \sum ((\sigma_i \cdot \sigma_j) \cdot (\sigma_k \cdot \sigma_l) + (\sigma_i \cdot \sigma_l) \cdot (\sigma_j \cdot \sigma_k) - (\sigma_i \cdot \sigma_k) \cdot (\sigma_j \cdot \sigma_l)))$$

All exchange coefficients J are positive

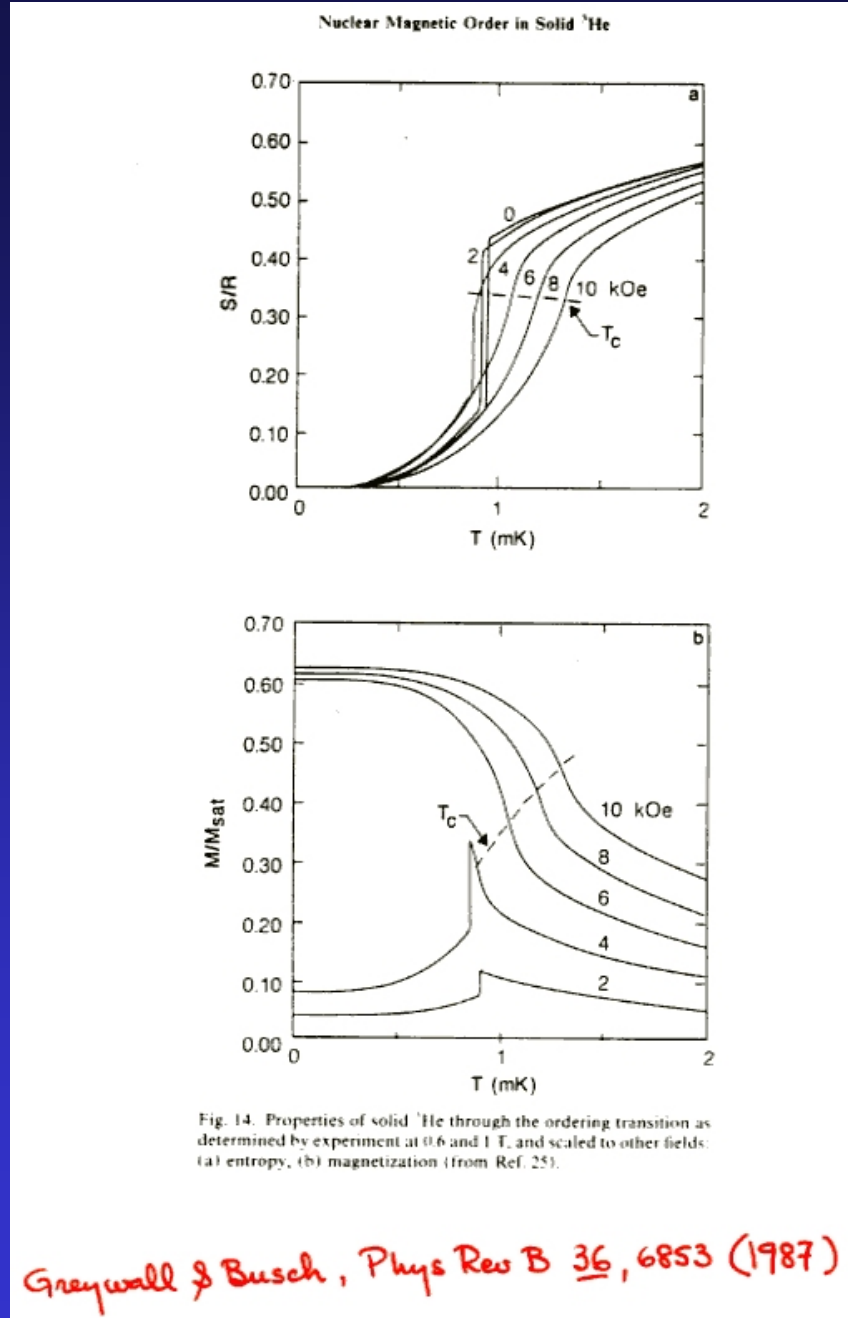
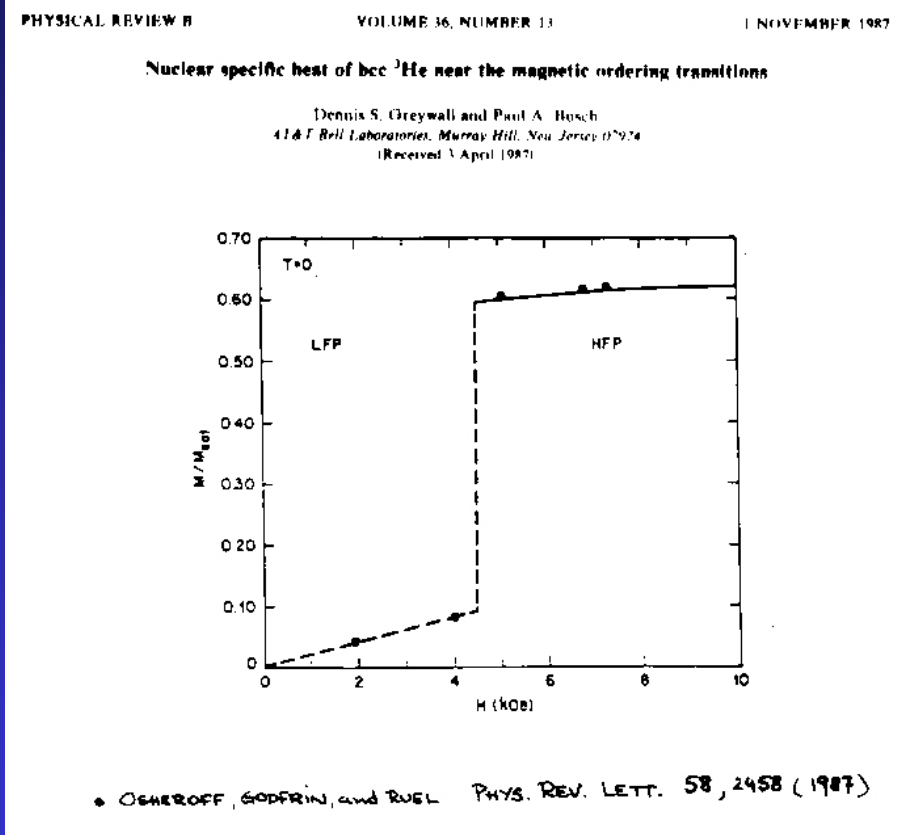
Nuclear order: U2D2 phase



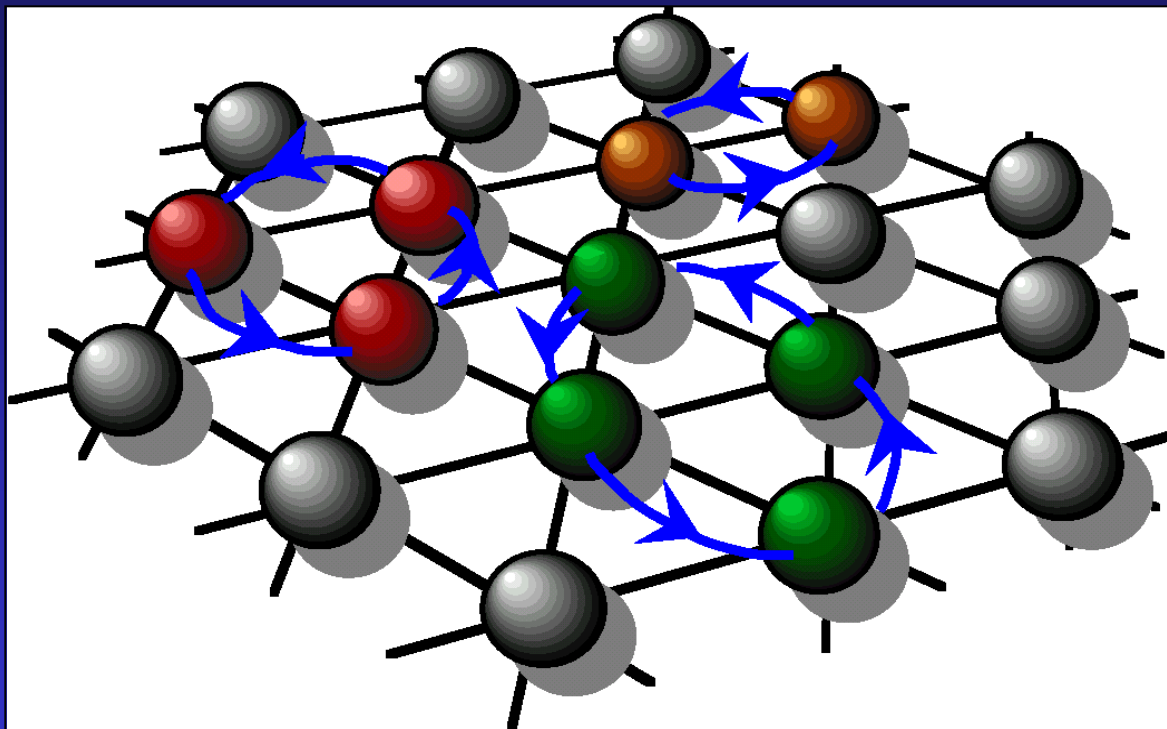
Nuclear order: CNAF phase



Heat capacity



Multi-spin exchange in 2D



2D Heisenberg Ferromagnet

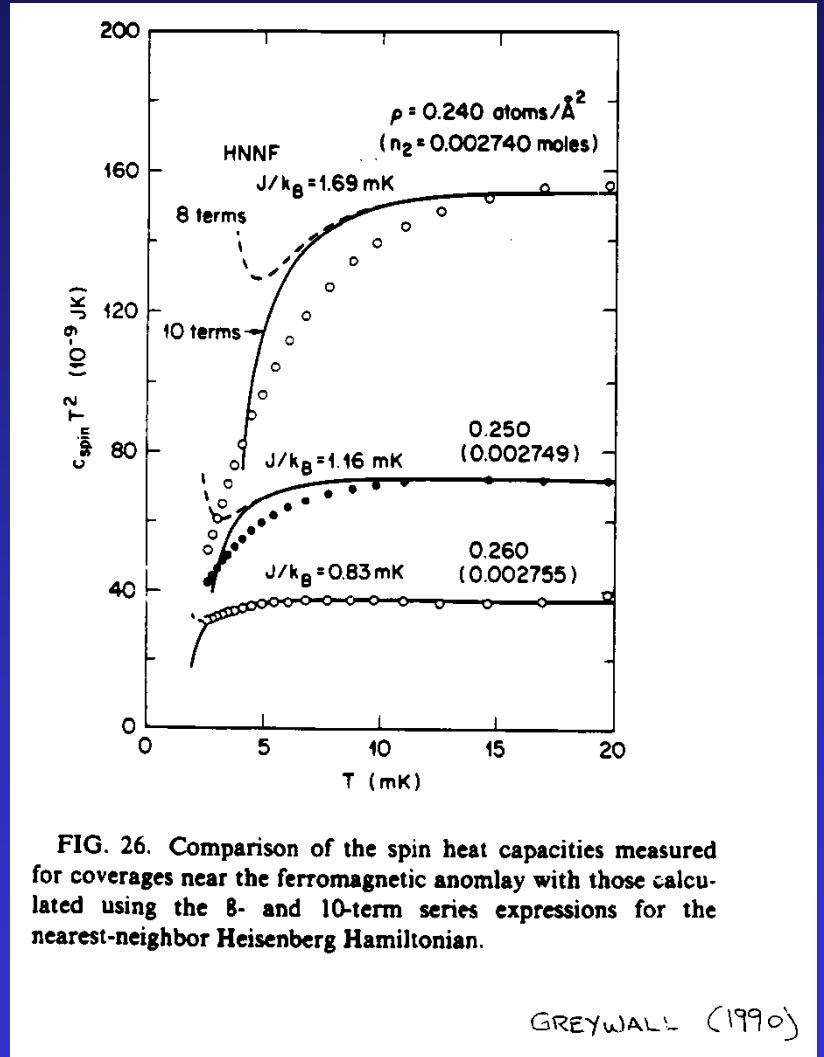
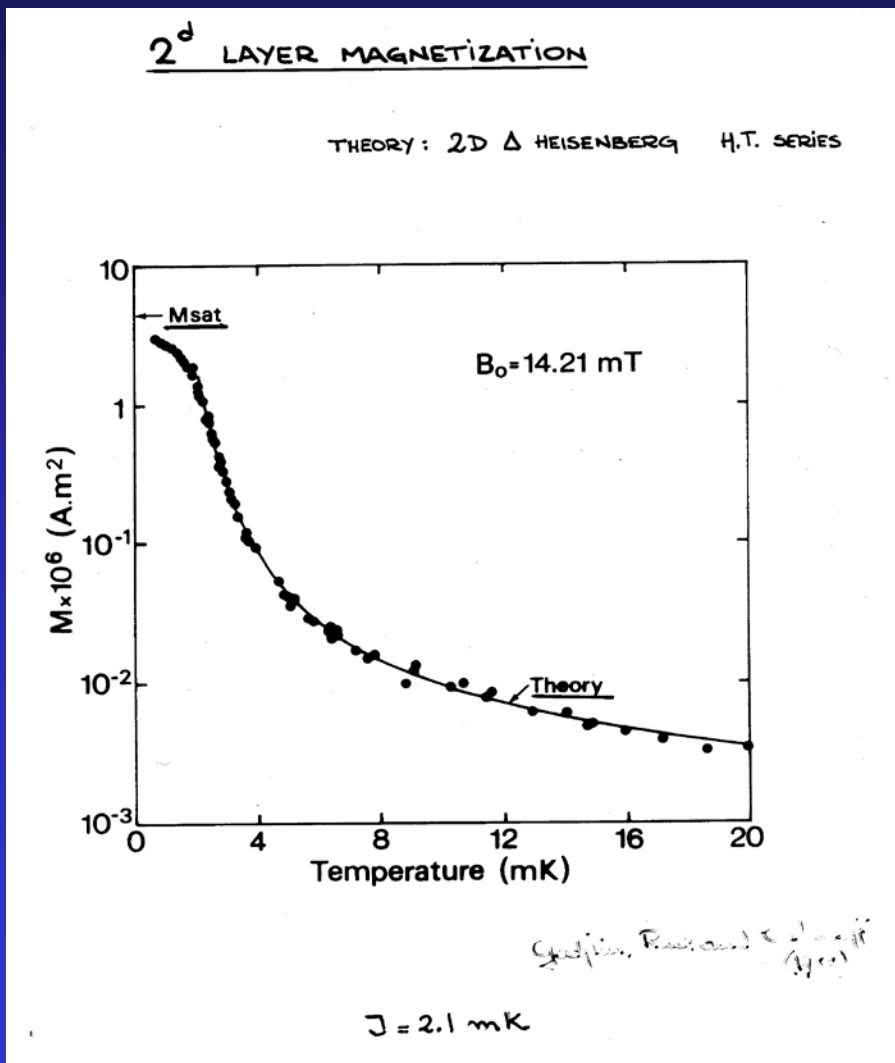


FIG. 26. Comparison of the spin heat capacities measured for coverages near the ferromagnetic anomaly with those calculated using the 8- and 10-term series expressions for the nearest-neighbor Heisenberg Hamiltonian.

GREYWALL (1990)

Spin-liquid phase

VOLUME 79, NUMBER 18

PHYSICAL REVIEW LETTERS

3 NOVEMBER 1997

Low Temperature Heat-Capacity Anomalies in Two-Dimensional Solid ^3He

K. Ishida, M. Morishita, K. Yawata, and Hiroshi Fukuyama*

Institute of Physics, University of Tsukuba, Tsukuba, Ibaraki 305, Japan
(Received 11 July 1997)

The heat capacity of second-layer solid ^3He adsorbed on graphite has been measured down to extremely low temperatures below $100 \mu\text{K}$. We observed a double-peak structure for a low-density registered solid, which strongly suggests that the system is a highly frustrated spin-1/2 two-dimensional (2D) antiferromagnet with a disordered ground state. As the density increases it approaches a 2D nearest-neighbor Heisenberg ferromagnet with a single rounded peak, which can be explained semiquantitatively by considering higher-order exchange processes up to six-spin exchange. (S0031-9007(97)04414-1)

PACS numbers: 67.70.+n, 67.80.Jd, 75.10.Jm, 75.70.Ak

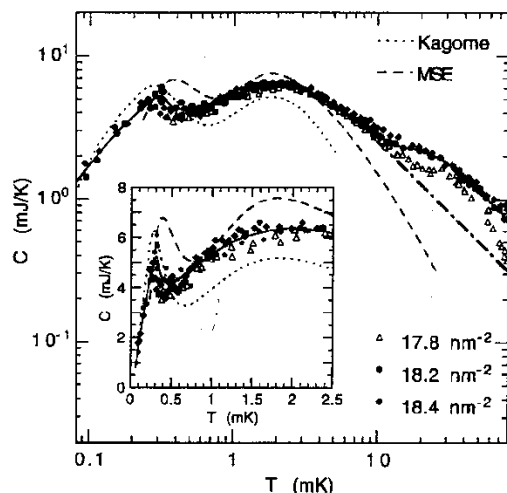


FIG. 1. Heat-capacity data at densities near the second-layer solidification. The solid line is a guide for the eye for the data at 18.2 nm^{-2} . The dotted line is from the Kagome model ($J = 2.59 \text{ mK}$; Ref. [2]). The dashed line is from the MSE model ($J = -3.23 \text{ mK}$, $J_4 = J_6 = 0.81 \text{ mK}$; Ref. [3]). The exchange parameters were determined so that the first-peak temperatures coincide with the experiment. Note that three quarters of N_2 are assumed to contribute to the spin heat capacity in the Kagome model (see text). The dash-dotted line is proposed true high-temperature behavior. The inset shows a linear plot of the low-temperature data.

VOLUME 86, NUMBER 11

PHYSICAL REVIEW LETTERS

12 MARCH 2001

Quantum Frustration in the “Spin Liquid” Phase of Two-Dimensional ^3He

E. Collin,¹ S. Triqueneaux,¹ R. Harakaly,^{1,2} M. Roger,³ C. Bäuerle,¹ Yu. M. Bunkov,¹ and H. Godfrin^{1,*}

¹Centre de Recherches sur les Très Basses Températures, Centre National de la Recherche Scientifique, BP 166, 38042 Grenoble Cedex 9, France

²Department of Experimental Physics, P.J. Šafárik University, Park Angelinum 9, 04154 Košice, Slovakia

³Service de Physique de l’Etat Condensé, Commissariat à l’Energie Atomique, Centre d’Etudes de Saclay, 91191 Gif sur Yvette, France
(Received 6 September 2000)

We have measured the ultralow temperature and low field magnetic susceptibility of the $\frac{4}{7}$ phase of two-dimensional ^3He adsorbed on graphite preplated by one layer of ^4He . The experiments are performed by progressively adding ^4He to the system, thus suppressing in a controlled way the ^3He atoms trapped in substrate heterogeneities. This procedure enables us to determine the intrinsic properties of this spin $\frac{1}{2}$ model magnet in the zero field limit. The results show quantitatively that the system is strongly frustrated by multiple spin exchange interactions. A characteristic gapped spin liquid behavior is observed at ultralow temperature.

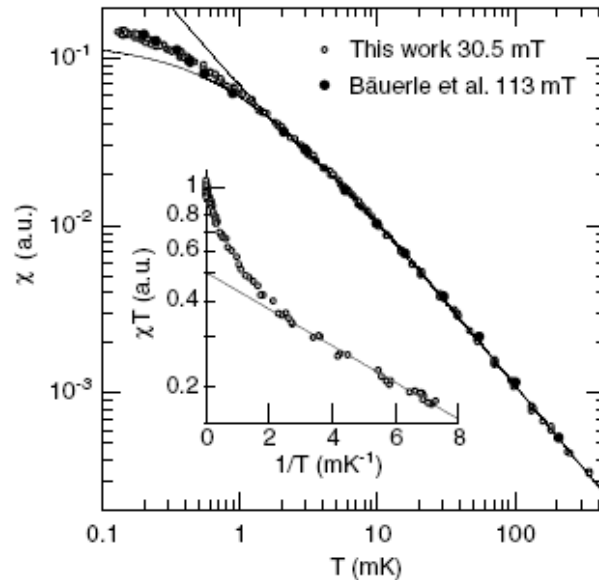


FIG. 3. Magnetic susceptibility of the pure $\frac{4}{7}$ phase. The solid lines correspond to the [2,3] Padé approximant of the HTSE of the MSE Hamiltonian [23] (upper curve), and to a Curie-Weiss fit (lower curve). The inset emphasizes the low temperature behavior of the susceptibility multiplied by temperature. The solid line shows an exponential decrease.

Conclusions

- Quantum fluids constitute interesting, simple, quantum many-body systems
- Elementary excitations
- Superfluidity
- Crystallisation
- Magnetism
- Supersolidity?